

## Review

## Electrical stimulation and piezoelectric biomaterials for bone tissue engineering applications

Deepak Khare <sup>a</sup>, Bikramjit Basu <sup>b,\*</sup>, Ashutosh Kumar Dubey <sup>a,\*\*</sup><sup>a</sup> Department of Ceramic Engineering, Indian Institute of Technology (BHU), Varanasi, 221005, India  
<sup>b</sup> Materials Research Center, Indian Institute of Science, Bengaluru, 560012, India

## ARTICLE INFO

**Keywords:**  
 Piezoelectric  
 Perovskites  
 Polarization  
 Electrical stimulation  
 Processing

## ABSTRACT

Bioelectrical phenomenon in natural bone has been well recognized for its role in bone development and fracture healing. For example, the piezoelectricity induced modulation in cellular functionality assists in the repair and regeneration of bone tissue. Against this backdrop, we review here the origin of dielectric and electrical responses (piezo-, pyro- and ferro-electricity) of natural bone along with their consequences in regulating the bone metabolic activities. The concept of piezoelectricity induced osteogenesis has driven the development of piezomaterials for bone regeneration applications. A number of recent studies have been critically analyzed to demonstrate as to how the surface charge polarization or electric field stimulation together with functional properties of piezoelectric biomaterials can synergistically modulate cell functionality, *in vitro* or tissue regeneration, *in vivo*. The examples are drawn from a range of piezoelectric bioceramics, (e.g. barium titanate, magnesium silicate etc.) and biopolymers (e.g. polyvinylidene fluoride (PVDF), collagen, etc). The challenging problem of processing the compositionally tailored bioceramics is emphasized in particular reference to (Na, K) NbO<sub>3</sub>, an implantable biomaterial with the most attractive combination of piezoresponsive properties. Taken together, this review comprehensively emphasizes the appealing relevance of piezo-bioceramics and piezo-biopolymers as next-generation orthopedic biomaterials.

## 1. Introduction

Bioelectrical cues of natural living bone, such as, piezoelectricity, pyroelectricity and ferroelectricity, etc. have been reported as some of the key factors in regulating metabolic activities like growth, structural remodeling as well as fracture healing [1–5]. The non-centrosymmetry of the collagen molecule has been suggested as the primary reason for the bioelectricity in living bone [1,2,5–8]. The endogenous electric field of living bone also helps in governing cell metabolism, such as, growth and proliferation, differentiation, motility, etc [9]. For example, human tibia generates a piezoelectric potential of about 300 µV during walking [10].

The application of physiological compressive loads increases the negative charges due to piezoelectric potential in bone [6,11]. These negative charges promote the functionality of osteoblast cells and consequently, enhance the bone regeneration [6]. However, low mechanical pressure results in reduced neo-bone formation as compared to higher pressure [12,13]. The fractured region of living bone becomes

more electronegative than the other regions [12,14]. As mentioned above, the generation of these negative charges promotes the activity of osteoblast cells, which help in matrix mineralization at the fractured site [6,11]. It can, therefore, be suggested that piezoelectric stimulation plays an important role in controlled bone regeneration.

The piezoelectric collagen in bone also develops streaming potential under stress, which results in the reduction of hydraulic permeability as well as an increase in stiffness [15]. Apart from piezoelectricity, biological response of hard tissues can also be improved by direct electrical stimulation [16–26].

The stress induced potential in piezo-bioceramics and piezo-biopolymers augments bone metabolism [27–32]. Piezoelectric bioceramics have already been demonstrated as sources of *in vivo* energy for biosensors and pacemakers [33,34]. Piezo-bioceramics/biopolymers develop surface electrical charges under the application of external stress, similar to bone [Fig. 1(A) and (B)] [35, 36, 37]. The polarized piezoelectric surfaces are reported to improve the osteogenic performance of natural bone [38–42]. Piezoelectric implants can potentially

\* Corresponding author.

\*\* Corresponding author.

E-mail addresses: [bikram@iisc.ac.in](mailto:bikram@iisc.ac.in) (B. Basu), [akdubey.cer@iitbhu.ac.in](mailto:akdubey.cer@iitbhu.ac.in) (A.K. Dubey).

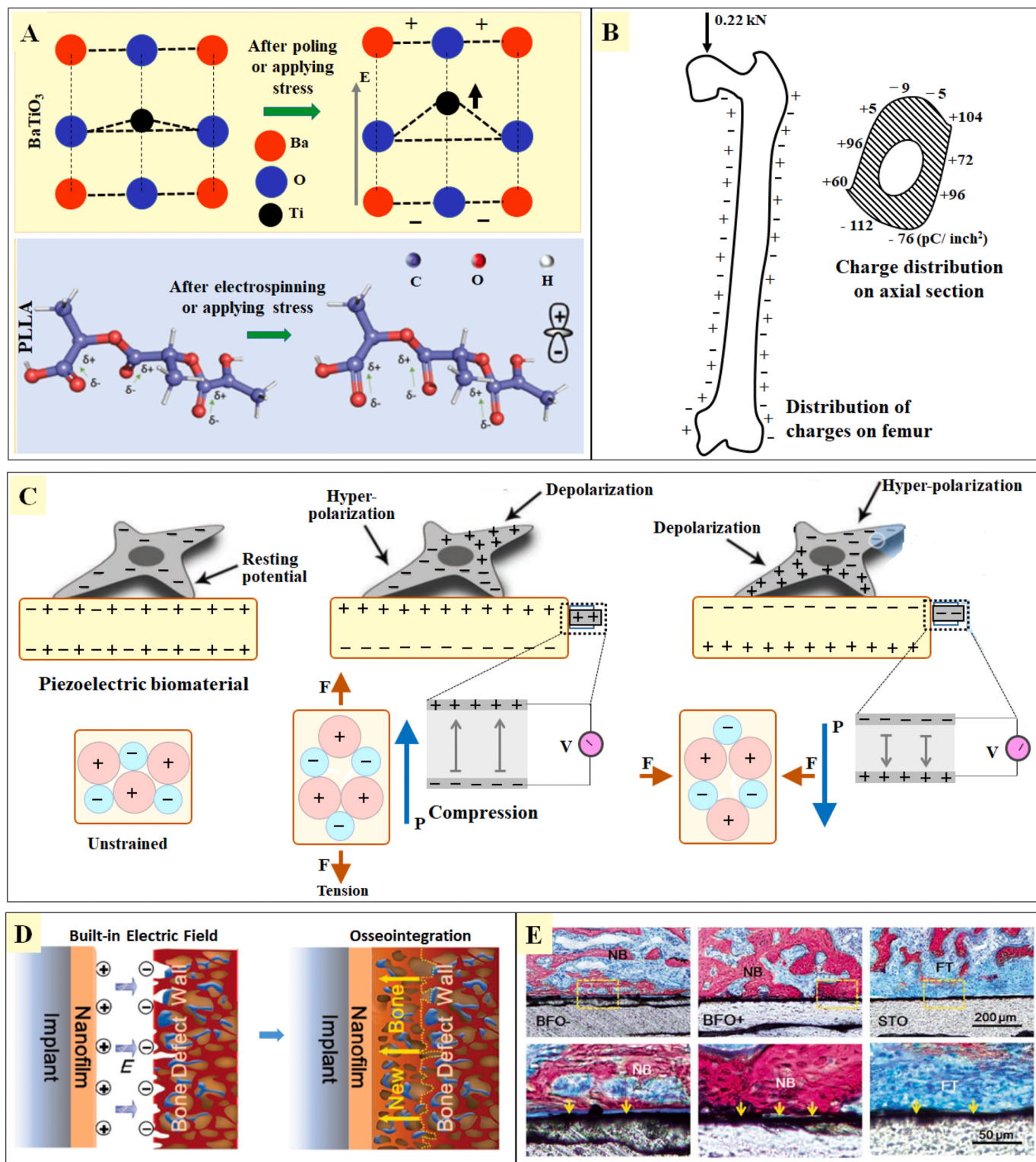


**Fig. 1. Stress generated electrical charges in natural bone and piezoelectric biomaterials induce endogenous cellular potential and facilitate bone formation.** (A) Schematic demonstration of generation of aligned dipoles or surface charge on piezoelectric ceramic ( $\text{BaTiO}_3$ ) and polymer poly-l-lactic acid (PLLA) with the application of mechanical stress, similar to human bone (Reproduced with the permission from publisher, Ref. [35]). (B) Stress generated surface electrical charge on the circumference of human femur (Reproduced with the permission from publisher, Ref. [37]). (C) Schematic illustration of the generation of surface electrical charge on strained piezoelectric material and resulting hyper-polarization/depolarization of cellular membrane (Reproduced with the permission from publisher, Ref. [43]). (D) Schematic representation of built-in electric field between positively charged nanocomposite and negatively charged bone wall, which enhances the osseointegration (Reproduced with the permission from publisher, Ref. [45]). (E) Histological evidences demonstrating significant neobone formation on the positively charged implant, when compared to negatively charged and uncharged implant (Yellow dotted block: implant-tissue interface, NB: nascent bone, FT: fibrous tissue, BFO:  $\text{BiFeO}_3$ , STO:  $\text{SrTiO}_3$ ) (Reproduced with the permission from publisher, Ref. [45]). (For interpretation of the references to colour in this figure legend, the reader is referred to the Web version of this article.)

promote bone fracture repair [40,42]. The implantation of piezoelectric scaffolds at the damaged site of the bone defect, develop stress generated electrical stimuli through physiological loads [Fig. 1 (C)] [43]. Such hyperpolarization activates voltage-gated calcium channels of the cell membrane [40]. The intracellular  $\text{Ca}^{2+}$  ions play an important role in cell proliferation [44]. It can, therefore, be inferred that piezoelectric biocompatible scaffolds result in an early repair of damaged tissue as compared to their non-piezoelectric counterparts [40]. For example, Liu

et al. [45] compared the osseointegration of positively polarized  $\text{BiFeO}_3$  (+BFO) membrane – strontium titanate (STO), negatively polarized BFO membrane – STO implant and non-polarized STO implant by the fixation in rat femur. A built in or integral electric field [Fig. 1 (D)] develops at the interface of oppositely charged + BFO-STO (+75 mV) and electro-negative bone defect surface (-52 to -87 mV) [45,46], which consequently promote more osseointegration as compared to -BFO-STO and non-polarized STO surfaces [Fig. 1 (E)].

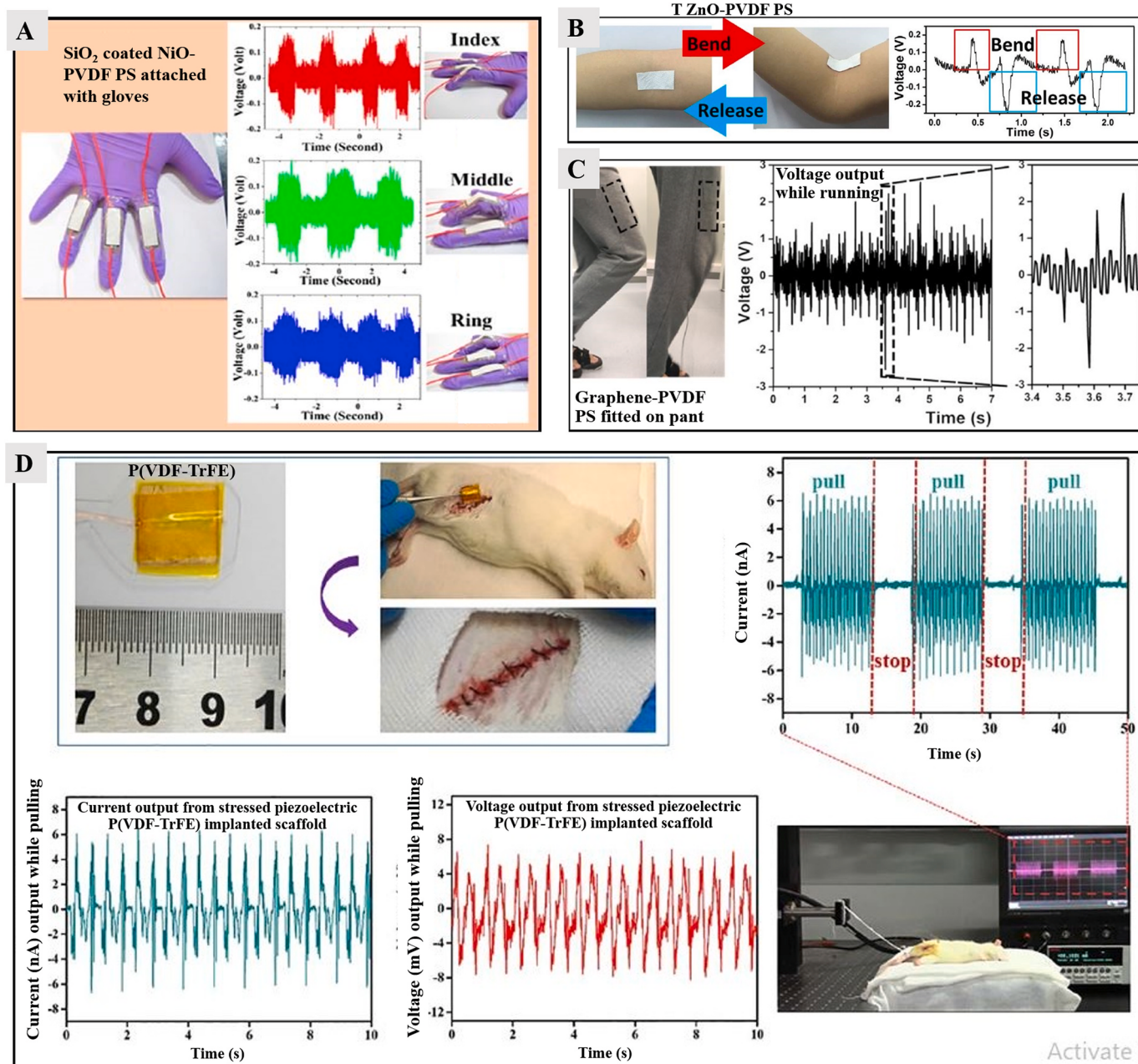


**Fig. 2. Piezoelectric potential, generated from natural bone during regular physiological activities.** [(A), (B) and (C)] PVDF based piezoelectric sensors (PS) as detectors of human activity in terms of piezoelectricity induced voltage output. [D] P(VDF-TrFE) based piezo-polymers (nanogenerator) implanted in the thigh of Sprague Dawley rat, mimicking piezoelectric potential generation during the regular activity. (A) PS nanocomposite, fabricated with PVDF/SiO<sub>2</sub> coated NiO assembled with gloves to determine the piezoelectric voltage output variation during stretching and bending movement of index, middle and ring fingers (Reproduced with the permission from publisher, Ref. [47]). (B) A PS nanocomposite with tetrapod ZnO/PVDF/polyester fabric, attached with elbow, to evaluate the amount of voltage output during bending and release (Reproduced with the permission from publisher, Ref. [48]). (C) A PS fabricated with PVDF/graphene in polyester fabric attached with marked region to determine the voltage output variation during running (Reproduced with the permission from publisher, Ref. [49]). (D) Electrospun P(VDF-TrFE) nanoscaffold implanted in the thigh of Sprague Dawley rat. The leg of rat was pulled up and released through a motor (bottom-right) and resulting variation in current output are shown (top-right) during pulling and releasing. The current and voltage output are also shown in bottom-left and bottom-middle graphs, respectively, in the pulling condition of rat's leg (Reproduced with the permission from publisher, Ref. [50]).

**Fig. 2(A)** and **(B)** and **(C)** illustrate the piezoelectric voltage generation from human bone during our routine activities [47–49]. For this purpose, piezoelectric sensors were embedded with skin, which was then subjected to stress during bend-release of fingers and elbow, during running etc. Positive and negative voltages were produced during bending and releasing of fingers, elbow and knee. Wang et al. [50] experimentally evaluated stress generated electrical potential from the implanted piezoelectric P(VDF-TrFE) scaffold during daily activities of Sprague Dawley rat [Fig. 2 (D)]. At the pulling condition of rat's leg, the peak output current and voltage from the strained implanted piezoelectric scaffold were recorded as 6 nA and 6 mV, respectively. Therefore, it can be suggested that the piezoelectric scaffold, implanted in the wounded site, generates electrical potential under physiological loads. This further stimulates osteoblastic activity and consequently, promotes bone regeneration in the wounded region.

Against the above backdrop, the present review describes the fundamentals, origin as well as consequences of piezoelectricity, pyroelectricity, and ferroelectricity in natural bone. Further, the potentiality of various piezoelectric bioceramics and biopolymers in mimicking such an electromechanical response of living bone has been revealed. Towards this end, the processing-related challenges to meet the desired piezoresponsive property combination have been discussed along with the possible combinations of remedies. In addition, the advantageous effects of polarized piezoelectric substrates in augmenting the biocompatibility have been discussed objectively.

### 1.1. The electroactive response of natural bone

Natural bone is a polymer aided ceramic hybrid composite. It carries inorganic and organic components of about 65 wt % and 25–30 wt %, respectively of the total bone mass [5,51]. The living bone generates electrical signals by the application of mechanical stress due to the presence of piezoelectric collagen [7]. These bioelectric signals stimulate bone growth [1,4,5]. The natural living bone has also been demonstrated to be a source of pyroelectricity [3,8] as well as ferroelectricity [2]. The electrical stimulation due to inherent bioelectricity of bone helps in bone repair [52] and the treatment of bone-related diseases, such as osteoporosis [53], bone tumor [54], etc.

### 1.2. Dielectric behavior

The dielectrics are electrically insulating materials with the ability to generate dipoles by the relative motion or separation between positive and negative charges, in the absence or presence of an external electric field. This is termed as polarization. The polarizability of a dielectric material in response to external electrical stimulation is measured in terms of dielectric constant.

In natural living bone, the hydrogen bond in collagen and HA is responsible for its polarizability [55]. The dielectric behavior of bone depends on the frequency and moisture content [56–58]. The dielectric constant of dry human bone has been reported to be about 10 over the frequency range of 1–100 kHz [55, 59, 60]. Dielectric relaxations in mineralized and demineralized bone were observed at relaxation frequencies of about 400 MHz and 200 MHz, respectively [56]. In demineralized bone, the reduction of calcium ions gives rise to the mobility of polar side chains in collagen fiber and results in lower relaxation frequency of demineralized bone [56]. The alternating current (AC) and direct current (DC) conductivity at 1 kHz of dry human femur has been reported to be of the order of  $10^{-10} (\Omega\text{-cm})^{-1}$  [57,60]. There is an interconnection among elastic modulus, mineral density and dielectric properties of bone, which suggests that the degradation in mechanical performance of bone can be monitored by measuring their electrical conductivity [53,61].

### 1.3. Piezoelectric response

The piezoelectricity is associated with the class of materials, where the application of mechanical stress results in the electrical polarization (direct piezoelectricity) and vice-versa (indirect piezoelectricity) [62, 63]. The piezoelectric crystals are anisotropic in nature. In the case of direct piezoelectric effect, the expression for induced polarization can be given as,  $P = d S$ , where,  $d$  and  $S$  are piezoelectric strain coefficient and applied stress, respectively. However, for indirect (converse) piezoelectric response, the expression for the piezoelectric strain is,  $\varepsilon = d E$ , where,  $\varepsilon$ ,  $d$  and  $E$  are strain, piezoelectric strain coefficient, and electric field, respectively.

The natural bone is piezoelectric in nature with collagen molecules being the origin of piezoelectricity [1,64]. The slipping of collagen fibers over each other under the application of mechanical force is specifically the cause of piezoelectricity in natural bone [65]. During physical activities like walking, stretching, climbing, etc., the collagen fibers undergo various kinds of movements like rotation, slipping, etc. and consequently, bone is subjected to stresses, like compression, tension, etc. [66]. Piezoelectric collagen leads to the development of charges in response to such kind of stresses [7]. The polarity of these electrical charges depends on the direction of mechanical stress or bone deformation [11]. Compression and tension generate negative and positive charges, respectively. Halperin et al. [7] reported the value of piezoelectric strain coefficient in human tibia to vary in the range of 7.7–8.7 pC/N. The lack of considerable scatter in piezoelectric strain coefficients indicates that the piezoelectric property is uniform across the bone.

### 1.4. Pyroelectricity

The ability of a material to polarize in response to any temperature change is measured in terms of pyroelectricity. Such polarization results in the generation of temporary voltage across the crystal. Natural bone shows pyroelectricity due to the presence of collagen [3,8]. Ramachandran et al. [67] proposed that the triple helix model of collagen, which consists of three parallel helical shaped chains, where each chain contains three amino acid residues per turn. The mutual conversion between lighter and heavier residues results in the distortion in triple helix structure of collagen, which renders pyroelectricity to natural living bone [67]. The pyroelectric coefficient of a human femur has been reported to be around  $0.0036 \pm 0.0021 \mu\text{C}/\text{m}^2\text{K}$  (in the temperature range of  $-25^\circ\text{C}$ – $60^\circ\text{C}$ ) [8].

### 1.5. Ferroelectricity

Ferroelectrics exhibit reversible spontaneous polarization and hysteresis loop. The collagen fibers, present in bone tissue, change their orientation in different directions from one plate to another plate, similar to the typical ferroelectric domain alignment [2]. The presence of hysteresis loop and permanent dipoles in bone structure confirms that ferroelectricity is a fundamental characteristic of natural bone. Hastings et al. [68] further confirmed the existence of permanent dipoles as well as remnant polarization ( $P_r = 0.00068 \mu\text{C}/\text{cm}^2$ ) in the bone. These dipoles can change their orientation under an external electric field, which is the reflection of reversible spontaneous polarization in natural bone.

## 2. Overview of piezoelectric biomaterials

Among various biomaterials, piezoelectric bioceramics, such as, sodium potassium niobate ( $\text{Na}_x\text{K}_y\text{NbO}_3$ , where,  $0 \leq x \leq 0.8$ ;  $0.2 \leq y \leq 1$ ; NKN) [69] or NKN-based ceramics [70,71],  $\text{BaTiO}_3$  [5,38,72–74], lithium sodium potassium niobate [75–77],  $\text{LiNbO}_3$  [78,79],  $\text{MgSiO}_3$  [80–82],  $\text{KNbO}_3$  [83],  $\text{ZnO}$  [44], boron nitride [84], bismuth ferrite ( $\text{BiFeO}_3$ ) [85] are reported to demonstrate reasonable potentiality to be prospective electroactive prosthetic implants. Similar examples from the class of piezoelectric biopolymers include polyvinylidene fluoride

(PVDF) [42], poly-L-lactic acid (PLLA) [86], polyhydroxybutyrate (PHB) [87], polyamides (Nylons, peptides, etc.) [88], polysaccharides (cellulose, chitosan, etc.) [89, 90, 91], collagen [92], etc. The dielectric, piezoelectric, ferroelectric, pyroelectric and electromechanical properties of the above mentioned piezoelectric bioceramics/biopolymers are summarized in Table 1 [7, 8, 29, 59, 60, 64, 68, 77, 79, 93, 94, 95, 96, 97, 98, 99, 100, 101, 102, 103, 104, 105, 106, 107, 108, 109, 110, 111, 112, 113, 114, 115, 116, 117, 118, 119, 120, 121, 122, 123, 124, 125, 126, 127, 128, 129, 130, 131, 132, 133, 134, 135, 136, 137, 138]. The piezoelectricity of the above materials is associated with their non-centrosymmetric structures. On the basis of the degree of symmetry or orientation, crystals can be classified into 32 crystal classes [62, 63]. Among 32 crystal classes, 21 classes possess non-centrosymmetric structures. Of these, one belongs to combined cubic symmetry and does not possess piezoelectricity, whereas, remaining 20 crystal classes exhibit piezoelectric phenomena. The 10 crystal classes, among these 20 non-centrosymmetric classes, develop polarization only by the application of mechanical stress and the remaining 10 crystal classes possess spontaneous polarization i.e., they possess piezoelectricity as well as pyroelectricity. A subgroup of these crystal classes demonstrates reversible spontaneous polarization which defines the ferroelectric behavior [62, 63].

As far as piezoelectric properties are concerned, NKN-based ceramics have been demonstrated among the best candidates, because of their reasonable piezoelectric strain coefficient ( $d_{33} = 260 \text{ pC/N}$ ), mechanical quality factor (240), high electromechanical coupling coefficient ( $k_{33} = 53\%$ ,  $k_p = 48\%$ ), and high Curie temperature ( $420^\circ\text{C}$ ) as well as relatively lower density ( $4.51 \text{ g/cm}^3$ ) as compared to other piezoelectric biocompatible materials [93, 139, 140, 141]. NKN has been patented as a potential biocompatible implant material, as they support the growth of human monocytes [69]. BaTiO<sub>3</sub> is another piezoelectric candidate with proven biocompatibility, *in vivo*. It has been demonstrated that BaTiO<sub>3</sub> promotes osteogenesis in dog femur bone [38, 72]. Below its Curie temperature ( $T_c = 120^\circ\text{C}$ ), BaTiO<sub>3</sub> possesses a polar asymmetric structure that imparts piezoelectricity [39]. This piezoelectricity in BaTiO<sub>3</sub> arises due to the slight relative displacement of the positively charged Ti<sup>4+</sup> ion ( $\sim 0.06 \text{ \AA}$ ) and negatively charged O<sup>2-</sup> ions ( $\sim 0.08 \text{ \AA}$ ) from the body and face centers, respectively, below the Curie temperature [142]. MgSiO<sub>3</sub>, with an asymmetric tetragonal structure, has been reported to be a good biocompatible piezoelectric substitute for bone, as testified by various *in vitro* and *in vivo* studies [80, 82, 143, 144]. MgSiO<sub>3</sub> is biodegradable, and the released Mg<sup>2+</sup> and Si<sup>4+</sup> ions stimulate osteogenic performance through the differentiation of mesenchymal stem cells into osteoblasts [144]. LiNbO<sub>3</sub> is another piezoelectric material, which has been suggested as a potential alternative for bone prosthesis [78, 79, 145]. LiNbO<sub>3</sub> possesses admirable ferroelectric (spontaneous

polarization;  $p_s = 78 \mu\text{C/cm}^2$ ), pyroelectric ( $p = 103.9 \mu\text{C/m}^2\text{K}$ ) and piezoelectric ( $d_{33} = 23 \text{ pC/N}$ ) properties [79, 101, 145]. Piezoelectric KNbO<sub>3</sub> is currently being used as a bio-probe for disease diagnosis and could be another alternative as an electroactive bone substitute [146, 147]. ZnO is another ceramic with reasonable piezoelectric ( $d_{33} = 12.4 \text{ pC/N}$ ) [108], pyroelectric ( $9.4 \mu\text{C/m}^2\text{K}$ ) [99] and dielectric ( $\epsilon = 12.27$ ) [108] potentials. ZnO also has the ability to generate piezoelectric potential, which results in enhanced cellular functionality and subsequently, promotes osteogenesis [44]. The piezoelectric boron nitride (BN) nanotubes, in its pristine as well as composite forms, have been reported to promote the proliferation and differentiation of mesenchymal stem cells [84]. Piezoelectric natural (proteins, polysaccharides, etc.)/synthetic (PVDF, PLLA, PHB, etc.) biopolymers are another class of emerging materials, that can be utilized for the regeneration of soft as well as hard tissues [27, 29, 89, 92].

Piezoelectric biomaterials and piezo-biopolymers are emerging biomaterials as next generation orthopedic implants. However, a number of processing concerns is to be addressed in synthesizing the consolidated stoichiometric composition of the above mentioned piezoelectric ceramics. For example, the volatilization of alkali elements (Na, K) restricts the high temperature processing and consequently, the densification of NKN-based ceramics by conventional processing techniques [139, 148–151]. To address such processing concerns, a number of approaches, such as use of sintering aids (to reduce the sintering temperature) [152–155], reduced atmosphere sintering [156, 157], advanced sintering routes, viz. cold isostatic pressing [76], hot pressing [158], hot isostatic pressing [159], spark plasma sintering [160], additive engineering [161–164] are being investigated.

### 3. Processing-related challenges for piezoelectric biomaterials: case of NKN

$\text{Na}_x\text{K}_{(1-x)}\text{NbO}_3$  (abbreviated as NKN for nominal composition) is a solid solution of ferroelectric KNbO<sub>3</sub> and anti-ferroelectric NaNbO<sub>3</sub> [165]. The alkali volatilization at the higher temperatures ( $>1000^\circ\text{C}$ ) and hygroscopic nature of alkaline carbonate precursors, especially  $\text{K}_2\text{CO}_3$  are the primary concerns associated with the processing of stoichiometric NKN-based ceramics [148]. The melting temperature of NaNbO<sub>3</sub> and KNbO<sub>3</sub> are about  $1420^\circ\text{C}$  and  $1040^\circ\text{C}$ , respectively [150, 166]. The consolidation, as well as microstructural control during high temperature sintering of NKN-based ceramics is difficult due to little difference between sintering and solidus temperatures [139, 149, 150]. For example, the solidus and liquidus temperatures for  $\text{Na}_{0.5}\text{K}_{0.5}\text{NbO}_3$  are about  $1140^\circ\text{C}$  and  $1280^\circ\text{C}$ , respectively [150].

In addition, a difference in diffusion rates of Na and K ions, with K<sup>+</sup> being the slowest diffusing species, retards the formation of

**Table 1**

A comparison of dielectric constants ( $\epsilon_r$ ), piezoelectric strain coefficients ( $d_{33}$ ), mechanical quality factors ( $Q_m$ ), remnant polarization ( $P_r$ ), electromechanical coupling coefficients ( $k_p$ ) and pyroelectric coefficients ( $p$ ) of various piezoelectric biomaterials with those of the natural bone.

Piezoelectric Biomaterials	$\epsilon_r$ (at 1–100 kHz)	$d_{33}$ (pC/N)	( $Q_m$ )	$P_r$ ( $\mu\text{C}/\text{cm}^2$ )	$k_p$ (%)	( $p$ ) ( $\mu\text{C}/\text{m}^2\text{K}$ )	Ref.
$\text{Na}_{0.5}\text{K}_{0.5}\text{NbO}_3$	657	160	240	31.4	44	–	[93, 94]
BaTiO <sub>3</sub>	1135	191	32	12.6	35	200	[95–99]
$\text{Li}_{0.06}(\text{Na}_{0.5}\text{K}_{0.5})_{0.94}\text{NbO}_3$	722.4	124	–	16.8	30.63	–	[77, 100]
$\text{LiNbO}_3$	62	23	–	–	–	103.9	[79, 101, 102]
MgSiO <sub>3</sub>	–	1.74 ( $d_{31}$ )	–	–	–	–	[103]
KNbO <sub>3</sub>	394	91.7	325	–	28	93	[104, 105]
ZnO	12.27	12.4	–	16.31	48 ( $k_{33}$ )	9.4	[99, 107–109]
BN	2–4	31.2 ( $d_{31}$ )	–	–	–	–	[110, 111]
PVDF	6–12	34	17.2	13	20 ( $k_{33}$ )	41	[112–118]
P(VDF-TrFE)	18	38	–	9.9	29 ( $k_{33}$ )	50	[113, 119–123]
PLLA	3–4	9.82 ( $d_{14}$ )	30.3	–	–	–	[29, 124, 125]
PHB	2–3.5	1.6–2 ( $d_{14}$ )	–	–	–	–	[29, 126, 127]
Polyamide	4–5	4 ( $d_{31}$ )	8.5	5.6–8.6	11	5	[29, 123, 128–131]
Collagen	2.6	0.2–2 ( $d_{14}$ )	–	0.29	–	0.12–0.37 @ $40^\circ\text{C}$	[132–135]
Chitosan	3.94	0.2–1.5 ( $d_{14}$ )	–	0.178	–	0.007	[132, 133, 136–138]
Human bone	9.2	7.50–9	–	0.00068	–	$0.0036 \pm 0.0021$	[7, 8, 59, 60, 64, 68, 106]

stoichiometric NKN [151]. The high vapor pressure of alkalis at higher temperatures ( $\sim 990^\circ\text{C}$ ) results in alkali phase reduction in NKN. The difference in equilibrium vapor pressures of K ( $P_{\text{K}} = 8 \times 10^{-3} \text{ Pa}$ ) and Na ( $P_{\text{Na}} = 3 \times 10^{-3} \text{ Pa}$ ) has also been suggested as one of the issues in the processing of stoichiometric NKN-based ceramics [167].

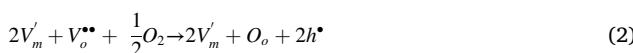
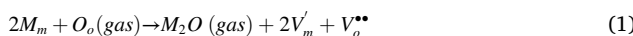
The alkali volatilization at higher temperatures results in the formation of secondary phases, such as,  $\text{K}_6\text{Nb}_{10.88}\text{O}_{30}$ ,  $\text{K}_2\text{Nb}_4\text{O}_{11}$ , etc. [168]. The sintering of NKN, above  $1000^\circ\text{C}$ , causes the formation of liquid phase due to the evaporation of  $\text{Na}_2\text{O}$ , which results in higher densification [149]. However,  $\text{Na}_2\text{O}$  evaporation results in the reduction of piezoelectric properties of NKN ceramics [149]. In order to control the evaporation of  $\text{Na}_2\text{O}$ , various sintering aids (low melting point oxides) such as, ZnO doped - CuO (sintering temperature,  $T_s = 900^\circ\text{C}$ ) [152],  $\text{V}_2\text{O}_5$  ( $T_s = 920^\circ\text{C}$ ) [153], (K, Na) - Germanate ( $T_s = 1000^\circ\text{C}$ ) [154],  $\text{Li}_2\text{O}$  ( $T_s = 1000^\circ\text{C}$ ) [155] etc. have been incorporated to reduce the sintering temperature of NKN-based ceramics. The addition of 5 mol. %  $\text{BaTiO}_3$  to the NKN specimen ( $0.95 \text{ Na}_{0.5}\text{K}_{0.5}\text{NbO}_3 - 0.05 \text{ BaTiO}_3$ ) has also been suggested as one of the ways to control  $\text{Na}_2\text{O}$  evaporation [149]. Such modification results in excellent piezoelectric properties ( $k_p = 36\%$ ,  $d_{33} = 225 \text{ pC/N}$ ) at relatively lower sintering temperature of  $1060^\circ\text{C}$  (2 h) [149].

The consolidation of NKN can also be improved by liquid phase sintering (LPS) [169], where sintering aids with the lower melting point are incorporated in NKN matrix phase to reduce the sintering temperature. It prevents alkali phase reduction, which consequently, enhances the densification of NKN-based ceramics. Therefore, the piezoelectric as well as electrical properties of NKN can be improved either by reducing the sintering temperature below  $1000^\circ\text{C}$  or by controlling the evaporation of  $\text{Na}_2\text{O}$  at higher temperatures ( $>1000^\circ\text{C}$ ). The important LPS aids for NKN includes, Cu, Zn, borate and germinate-based compounds [154,170–173]. Cu-based sintering aids are  $\text{K}_4\text{CuNb}_8\text{O}_{23}$  (0.5 mol. %),  $\text{K}_{5.4}\text{Cu}_{1.3}\text{Ta}_{10}\text{O}_{29}$  (0.38 mol. %), etc., which enhance the densification ( $>97.6\% \rho_{\text{th}}$ ) and piezoelectric properties ( $d_{33} = 180\text{--}190 \text{ pC/N}$ ,  $k_p = 39\text{--}42\%$ ,  $Q_m = 1200\text{--}1400$ ) of NKN-based ceramics, at relatively lower sintering temperatures ( $1095\text{--}1120^\circ\text{C}$ ) [170]. The addition of ZnO (1 mol. %) and  $\text{K}_{1.94}\text{Zn}_{1.06}\text{Ta}_{5.19}\text{O}_{15}$  (0.5 mol. %) has also been reported to provide improved densification (up to  $96.3\% \rho_{\text{th}}$ ) and piezoelectric properties ( $d_{33} = 123\text{--}126 \text{ pC/N}$ ,  $k_p = 40\text{--}42\%$ ,  $Q_m = 60\text{--}140$ ) of NKN-based ceramics [171,172]. Similarly, borate-based sintering aids such as, 0.45 wt % of borax or  $\text{Na}_2\text{B}_4\text{O}_7 \cdot 10\text{H}_2\text{O}$  ( $\rho_r = 95.5\% \rho_{\text{th}}$ ,  $d_{33} = 131.6 \text{ pC/N}$ ,  $k_p = 34.8\%$ ,  $Q_m = 109$ ) [173] and 1 wt % of germinate-based K, Na-germinate sintering aids ( $\rho_r = 95.6\% \rho_{\text{th}}$ ,  $d_{33} = 120 \text{ pC/N}$ ,  $k_p = 40\%$ ,  $Q_m = 77$ ) also contribute to the densification and piezoelectric properties of NKN-based ceramics [154].

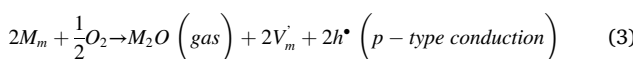
Kobayashi et al. [156,157] suggested that the sintering in reduced oxygen can effectively diminish the possibility of the volatilization of alkalis during the processing of NKN ceramics. Such processing results in relatively high dielectric constant ( $415.6$ ) and resistivity ( $2.70 \times 10^9 \Omega\text{-m}$ ) in NKN. In reduced atmosphere sintering, the energy for the formation of oxygen vacancies decreases and that of alkali vacancies increases. Consequently, oxygen vacancy increases and alkali (Na, K) vacancy decreases, which indicates a decrease in alkali volatilization.

Alkali volatilization during sintering in air as well as reduced oxygen atmosphere can be represented as [156,157],

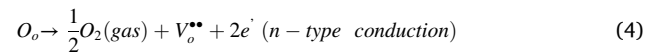
(a) In air atmosphere (p-type conduction),



The combination of equations (1) and (2) yields,



(b) In reduced oxygen atmosphere (n-type conduction),



where, M,  $V_m$ , and  $V_o$  indicate alkali metal, alkali metal and oxygen vacancies, respectively.

Li modified and hot-pressed [ $850\text{--}1150^\circ\text{C}$  at  $\sim 7\text{--}69 \text{ MPa}$  for 1 h] (Na, K, Li)  $\text{NbO}_3$  has been developed with excellent electromechanical coupling coefficient ( $k_p = 45\%$ ) [158]. The issues, associated with the consolidation of NKN-based ceramics have also been suggested to address via cold isostatic pressing (CIP) where, high pressure of about  $100\text{--}200 \text{ MPa}$  is applied to obtain highly dense ceramics with improved piezoelectric properties [76,161,162]. Despite significant porosity, the CIPed material has been demonstrated to possess reasonable piezoelectric properties ( $d_{33} = 117 \pm 6 \text{ pC/N}$ ,  $k_p = 24 \pm 3\%$ ). CIPed ( $200 \text{ MPa}$ ) NKN-based ceramics, modified with  $\text{BaTiO}_3$  (2 mol. %,  $T_s = 1100\text{--}1250^\circ\text{C}$ ),  $\text{LiNbO}_3$  (5–7 mol. %,  $T_s = 1040\text{--}1100^\circ\text{C}$ ),  $\text{LiTaO}_3$  (5–6 mol. %,  $T_s = 1110^\circ\text{C}$ ) or  $\text{SrTiO}_3$  (0.5–2%,  $T_s = 1100\text{--}1250^\circ\text{C}$ ) have been demonstrated to provide better densification ( $97\text{--}98.4\% \rho_{\text{th}}$ ) with reasonable piezoelectric properties ( $d_{33} = 96\text{--}235 \text{ pC/N}$ ,  $k_p = 29\text{--}44\%$ ) [161–164]. Sol-gel synthesized ( $\text{Na}_{0.52}\text{K}_{0.4425}(\text{Nb}_{0.8825}\text{Sb}_{0.08})\text{O}_3 - 0.0375 \text{ LiTaO}_3$ ) exhibits favorable piezoelectric properties ( $d_{33} \sim 418 \text{ pC/N}$ ,  $T_c \sim 257^\circ\text{C}$  and  $k_p \sim 54\%$ ), when consolidated by conventional sintering at  $1090^\circ\text{C}$  [141].

Spark plasma sintering (SPS) is one of the most emerging non-conventional routes of sintering to obtain highly dense ( $\sim 97\text{--}99.8\% \rho_{\text{th}}$ ) NKN-based ceramics, with excellent piezoelectric properties ( $d_{33} \sim 148\text{--}280 \text{ pC/N}$ ,  $k_p \sim 39\text{--}48\%$ ) [160,174,175]. The reduced sintering temperature suppresses alkali volatilization in NKN, which has very important consequences as far as the dielectric and piezoelectric properties are concerned.

Apart from non-conventional sintering routes, property enhancement with chemical modification is a multifaceted and economical technique for the improvement in densification as well as piezoelectric and electrical properties of NKN-based ceramics. Several additives have been reported that enhances the piezoelectric properties of  $\text{N}_{0.5}\text{K}_{0.5}\text{NbO}_3$  ceramics such as, 2 mol. %  $\text{BaTiO}_3$  ( $d_{33} = 104 \text{ pC/N}$  and  $k_p = 29\%$ ), 6 mol. %  $\text{LiNbO}_3$  ( $d_{33} = 235 \text{ pC/N}$  and  $k_p = 42\%$ ), 5 mol. %  $\text{LiTaO}_3$  ( $d_{33} = 200 \text{ pC/N}$  and  $k_p = 36\%$ ) and 2 mol. %  $\text{SrTiO}_3$  ( $d_{33} = 92 \text{ pC/N}$  and  $k_p = 26.6\%$ ) [161–164]. The improved piezoelectric properties are attributed to the formation of morphotropic phase boundary (MPB).

In addition, various non-conventional techniques and chemical modifications are in continuous thrust for the development of biocompatible ceramics with excellent piezoelectric properties. Several studies, reviewed in the upcoming sections, revealed that improvement in piezoelectric property of bioceramics and biopolymers results in better osteogenesis at the implant-tissue interface.

#### 4. Piezoelectricity and biocompatibility

Several studies suggest that the polarized piezoelectric bioceramics and biopolymers improve the osteogenesis through various ways [5,38, 69,70,73,77–79]. The electrical potential, induced in piezoelectric ceramics can potentially enhance the bioactivity and cellular response for hard tissue regeneration [Fig. 3] [17, 39, 42, 176, 177, 178].

##### 4.1. Origin of biominerization and cytocompatibility

*In vitro* biominerization study on polarized piezoelectric  $\text{BaTiO}_3$  ceramic demonstrated the deposition of calcium phosphate (CaP) layer on the negatively polarized surface, while no CaP layer was observed on

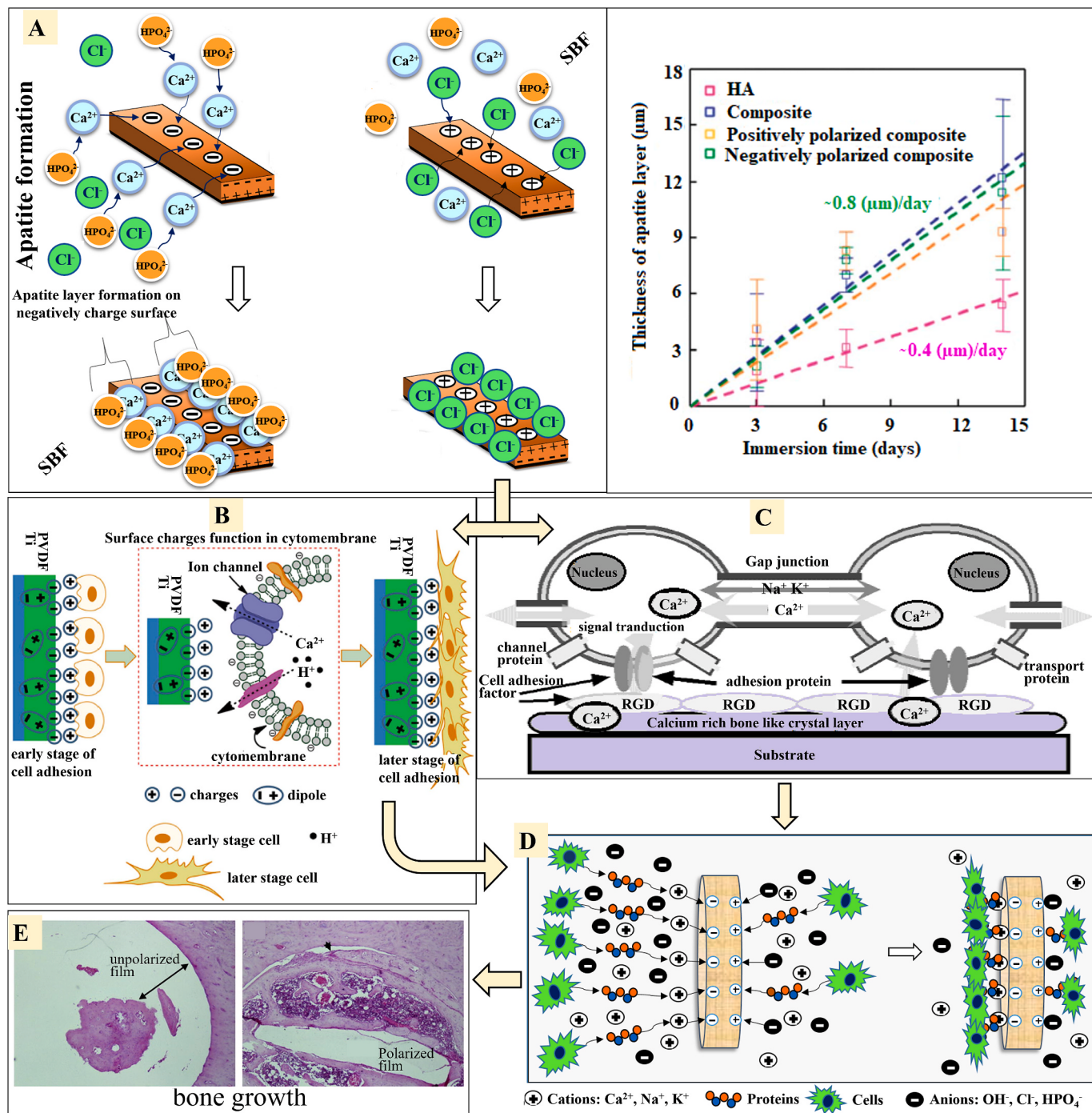


**Fig. 3. Surface polarization induced bioactivity and cellular response, *in vitro* and *in vivo*.** Polarized surface of piezoelectric materials promote the adsorption of apatite ions ( $\text{Ca}^{2+}$ ,  $\text{HPO}_4^{2-}$ ) or proteins and cell adhesion and consequent impact on hard tissue regeneration. (A) Schematic illustrating the mechanism of apatite formation on negatively charged surface as compared to the positively charged surface [39]. The polarization induced enhanced rate of apatite formation on HA-LNKN-HA functionally graded material (FGM) as compared to unpolarized FGM and HA (Reproduced with the permission from publisher, Ref. [178]). (B) Schematic representing the polarization induced enhanced osteogenesis. Cations (like  $\text{Ca}^{2+}$  ions and  $\text{H}^+$  ions) from the physiological environment are attracted towards the negatively charged PVDF-Ti surface. Consequently, these cations attract negatively charged cytomembrane (Reproduced with the permission from the publisher, Ref. [177]). (C) An illustration of neuroblastoma cell response on polarized HA surface.  $\text{Na}^+$  and  $\text{Ca}^{2+}$  work as neurotransmitters between two cells through gap junction.  $\text{Ca}^{2+}$  activates protein adhesion factors and consequently, enters into the cells through these adhesive proteins and moves towards the neighboring cell through gap junction (Reproduced with the permission from the publisher, Ref. [176]). (D) Schematic demonstration of the influence of surface polarity on the interaction between the sample surface and constituents of culture media such as cations, anions, proteins and cells [17,176]. Negatively charged surface attracts cations, followed by proteins as well as cells. Positively charged surface attracts anions, which inhibits the protein adsorption. (E) H & E stained images, representing the healing of defects (double arrow) on the unpolarized and polarized  $\beta$ -PVDF film, implanted in rat's femur for 4 weeks. Unpolarized  $\beta$ -PVDF implanted film could not exhibit neobone formation after 4 weeks of implantation; however, the defect on the polarized  $\beta$ -PVDF implanted film was about to be completely covered by bone marrow like spongy tissue and trabecular bone tissue after 4 weeks of implantation (Reproduced with the permission from the publisher, Ref. [42]).

the positively charged surface [Fig. 3 (A)] [39]. Due to electrostatic interaction between  $\text{Ca}^{2+}$  ions, present in simulated body fluid (SBF) and negatively charged surface, deposition of  $\text{Ca}^{2+}$  ions takes place on the polarized surfaces [39]. The anions ( $\text{HPO}_4^-$  and  $\text{OH}^-$ ), in turn, interact with these deposited  $\text{Ca}^{2+}$  ions and, form CaP layer on the negatively polarized surfaces [Fig. 3 (A)]. However,  $\text{Cl}^-$  ions, present in SBF are attracted towards positively charged surfaces, which do not support the formation of the CaP layer [39] [Fig. 3 (A)]. Similarly, it has been demonstrated that the negatively polarized surface of HA- Li modified (6 mol.%) NKN (LNKN)-HA functionally graded material almost doubled the rate of apatite formation [right part of Fig. 3 (A)] as compared to non-polarized monolithic HA [178]. Zhai et al. [177] elucidated enhanced cell proliferation on polarized Ti - 10 vol % polyvinylidene

fluoride (PVDF) polymer [Fig. 3 (B)]. The cations ( $\text{Ca}^{2+}$ ,  $\text{H}^+$  ions) from the biological fluid, adhere on the negatively charged surface. These cations further attract negatively charged proteins (like integrin, fibronectin) and cytomembrane. Consequently, the cell adhesion and proliferation on the negatively charged PVDF-Ti increase.  $\text{Ca}^{2+}$  ions, present in the apatite layer, activate cell adhesion factors [176] [Fig. 3 (C)]. Consequently,  $\text{Ca}^{2+}$  ions, adhered on the apatite rich polarized surface, enter into the cells and move towards the nearest cell [176]. Such kind of transportation of  $\text{Ca}^{2+}$  ions between the cells promotes the cell-cell adhesion and anchoring of cells on the CaP layer, formed on the negatively polarized ceramic surfaces [176]. Similarly, negatively polarized piezoelectric ceramics enhance the cell growth as compared to their positively polarized surfaces [Fig. 3 (D)] [17].

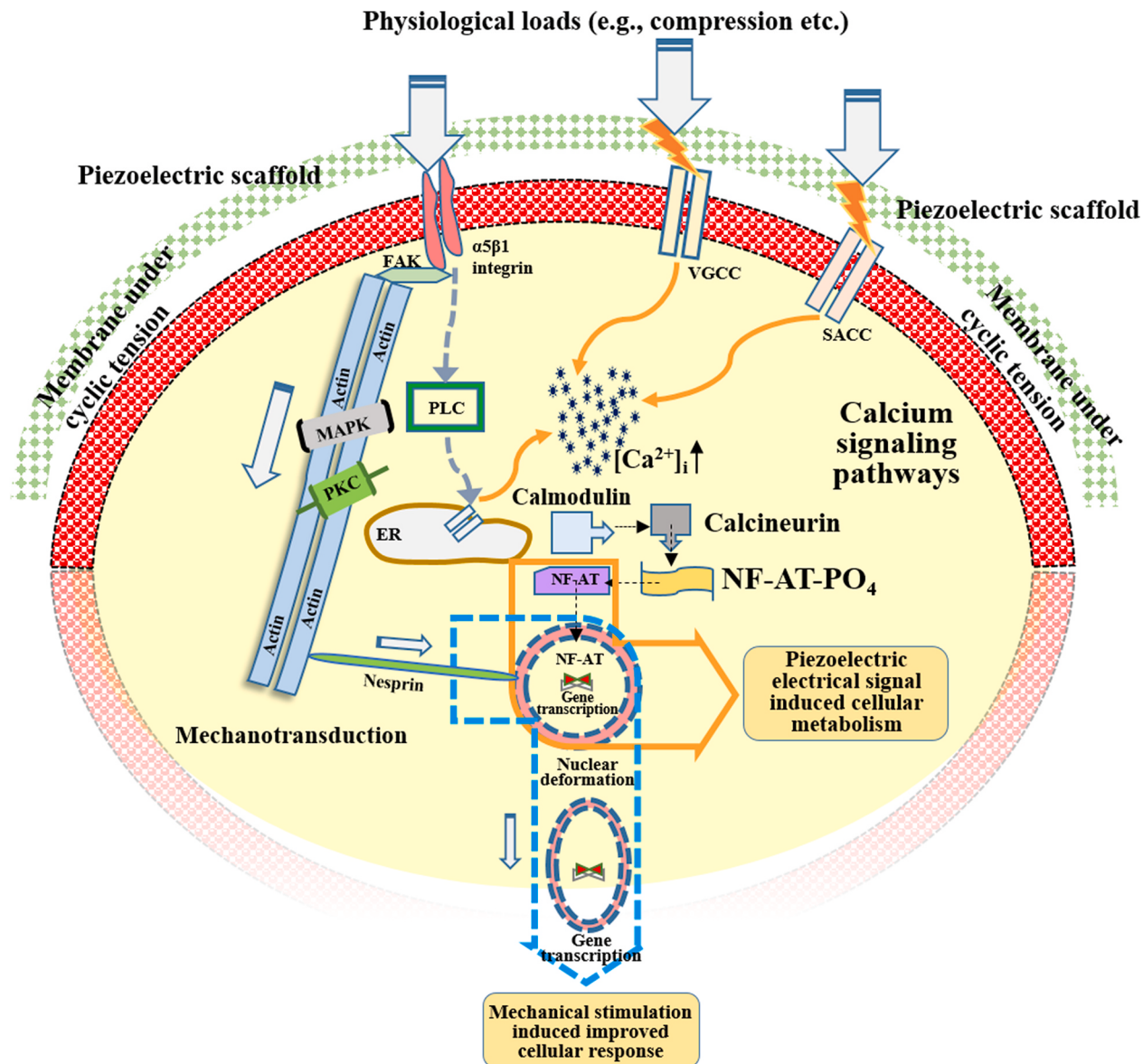


**Fig. 4. Schematic illustration of the effect of mechanical stimulation on cell metabolism through intracellular electrical signal transduction, leading to activation of mechanoreceptors [30,40,44,177].** Electromechanical signals facilitate outside-in  $\text{Ca}^{2+}$  ions influx through the opening of voltage gated  $\text{Ca}^{2+}$  channels (VGCC) and stretch activated calcium channels (SACC) [40,44]. Consequently, intracellular ions increase which activate the calmodulated protein and calcineurin [30,40]. These calcium activated calcineurin dephosphorylates the phosphorylated nuclear factor of activated cells (NF-AT) and shifts towards the nucleus, where it executes gene transcription [30,40]. Mechanically stimulated activated membrane receptors open up receptor channels and permit intracellular  $\text{Ca}^{2+}$  ions from endoplasmic reticulum calcium stores [40,44]. Also, physiological loads directly activate mechanoreceptors of the cell membrane like integrin, which actuate PKC (protein kinase C) and MAPK (mitogen activated protein kinase) signaling pathways [30,180,181]. These signaling cascade propagates towards the nucleus, where it interacts with mechanosensitive transcription factor and results in gene transcription [30,180,181]. NF-AT-PO<sub>4</sub>: Phosphorylated nuclear factor of activated cells, ER: Endoplasmic reticulum, FAK: Focal adhesion kinase, PLC: Phospholipase C.

As discussed above, the negatively polarized surface attracts cations like,  $\text{Ca}^{2+}$  ions present in the biological fluid, a phenomenon which serves as a stimulus for the adsorption of proteins and subsequently, promotes cellular adhesion [17,176]. However, positively charged surface attracts anions like  $\text{Cl}^-$ ,  $\text{OH}^-$ , etc, which restricts the adhesion of proteins as well as cells [17]. Apart from above mentioned *in vitro* response, *in vivo* assessment of unpolarized and polarized  $\beta$ -PVDF polymer samples was made by the implantation in rat's femur [42]. It has been observed that neo trabecular bone regeneration takes place on the polarized polymer samples after 4 weeks of implantation, which was almost absent in the case of unpolarized polymers of identical macromolecular chemistry, for the similar period (4 weeks) of implantation [Fig. 3 (E)]. The mechanical stimulus, induced by physiological loadings in rat's femur generates a voltage gradient on the polarized implant surfaces, which is responsible for the increased bone growth.

#### 4.2. Origin of bone healing

The damaged tissues can be healed by the piezoelectricity induced electrical stimulation as well as direct mechanical stimulation [30,40, 44,179]. These mechanisms can be elaborated through two independent moduli [Fig. 4]. According to the first module, piezoelectric scaffolds generate electrical potentials under the influence of functional loads. Such type of electrical stimulation activates voltage-gated  $\text{Ca}^{2+}$  channels and stretch activated calcium channels pathways, which results in an increase in intracellular  $\text{Ca}^{2+}$  ions [Fig. 4] [40,44]. In addition, the local electrical field can modify the configuration of membrane receptors and opens receptor channels, which allow an influx of intracellular  $\text{Ca}^{2+}$  ions from the endoplasmic reticulum [Fig. 4] [40,44]. These increased  $\text{Ca}^{2+}$  ions in cells activate calcium modulated proteins as well as calcineurin (a kind of calcium dependent protein phosphatase) [30,40]. These calcineurin proteins react with the phosphorylated nuclear factor of activated cells (NF-AT-PO<sub>4</sub>) and convert it into dephosphorylated nuclear factors of activated cells (NF-AT) [30,40]. These dephosphorylated NFs-AT translocate to the nucleus, where they combine with other proteins and result in gene transcription [Fig. 4]. Gene transcription promotes the synthesis of TGF- $\beta$  and BMP-2 and consequently, regulates cell metabolism and ECM synthesis [30,40].

According to second module, mechanical stimulation directly activates mechanoreceptors, such as integrins [30,180]. The activated integrins translocate protein kinase C (PKC) to the cell membrane and activate MAP Kinase (MAPK) pathways for transmembrane signaling [30,180] and consequently, transfer extracellular mechanical signals to actin [180]. RACK 1 protein (intracellular receptor) associated with integrin, binds with the PKC domain. Therefore, RACK1 mediated PKC-integrin interaction plays a key role in transmembrane signal transduction [30,180,181]. Now, these signaling cascades transfer towards the nucleus and interact with mechanosensitive transcription factors and consequently, execute gene transcription [30,180].

The polarized (at 13 kV for 30 min) piezoelectric BaTiO<sub>3</sub> - polymer [poly(vinylidene fluoride trifluoroethylene)] nanocomposite membranes demonstrated long lasting electrical charge storage capability. These biomaterials can facilitate the differentiation of rat bone marrow mesenchymal stem cells (rBMSCs) into osteoblast cells [28]. The implantation of such polarized piezoelectric biocomposite in the calvarial site defect of rat bone has been demonstrated to promote early bone regeneration [28].

The mechanical deformation of bone collagen induces both, negative (under compression) as well as positive (under tension) potentials due to piezoelectricity [15]. Natural bones possess inherent negative zeta potential (- 5 mV) [15]. The negative charges, developed due to the compression of bone collagen, increase the overall zeta potential as well as streaming potential in natural living bone [15]. This stress-stimulated electrical potential enhances the electroosmosis, and consequently, decreases the hydraulic permeability and increases the stiffness of bone [15].

The application of optimal electrical stimulation results in enhanced proliferation and differentiation of human mesenchymal stem cells on biomaterials surfaces, which subsequently, assists in bone repair and regeneration [16,17,21,24,25]. The cellular response can also be enhanced by improving the conductivity of the substrate surface in a controlled manner [25]. Apart from the improved cellular response, the application of electrical field with specific pulse rate results in electroporation, which can be utilized for cancer treatment [17,24]. Electrical stimulation can also control the directional movement of cells [25,27].

In absence of an electric field, a cell membrane exhibits negative potential. The application of a direct current electrical field (dcEF) hyperpolarizes the anodal side membrane of the cell [25,27]. Consequently,  $\text{Ca}^{2+}$  ions diffuse at the anodal side membrane of the cell. This increased amount of  $\text{Ca}^{2+}$  ions on the anode side results in depolymerization of actin, which causes shrinkage in cell size at the anodal end. At the same time, due to the depolarization at the cathode side membrane of the cell, the number of  $\text{Ca}^{2+}$  ions decreases, which causes the polymerization of actin and protrusion on this side of the cell. Such kind of changes in cell morphology promotes the cell movement towards the cathode side [25,27]. However, the depolarization of the cathode side membrane of the cell opens its voltage-gated  $\text{Ca}^{2+}$  channels and consequently, increases the amount of intracellular  $\text{Ca}^{2+}$  ions [25]. Therefore, the amount of  $\text{Ca}^{2+}$  ions on both, cathodal side (due to the influx of extracellular  $\text{Ca}^{2+}$  ions) and on the anodal side (due to diffusion), causes a net movement of cells either towards cathode side or anode side, where the number of  $\text{Ca}^{2+}$  ions are less [25]. Therefore, the direct current electrical field (dcEF) can control the net movement of the cells [25,27]. Such type of controlled cell locomotion through electrically modified endogenous charges leads to an increased attachment of cells on the wounded site that assists in wound healing. Such a phenomenon also prevents cellular accumulation on the cancerous site which is used in cancer treatment.

The efficacy of a number of piezoelectric bioceramics and biopolymers as a prospective substitute for electrically-active bone tissue is described in subsequent sections, which reveal the potentiality of piezoelectric materials as next generation materials for orthopedic implant applications.

#### 4.3. Biomaterials-based perspective

##### 4.3.1. NKN-based ceramics

Nilson et al. [69] examined the biocompatibility of NKN using human monocytes. Jalalian et al. [71] fabricated the dense ferroelectric NKN nanofibers with the help of sol-gel electro-spinning route and reported cube on cube growth of NKN nano-crystals in the crystallographic direction [001]. Such textural evolution in nanofibers suggested good potential of the electrically polarized NKN nanofibers as a scaffold for repair and regrowth of damaged/injured tissues [71]. The space charge on the polarized surfaces of NKN-based ceramics plays an important role in modulating the biological responses, such as protein adsorption, cell proliferation, etc. [70,76,77].

Chen et al. [70] reported that the polarized (@ 25 kV/cm) NKN increases protein adsorption on both, positively ( $0.43 \text{ mg}\cdot\text{cm}^{-2}$ ) as well as negatively ( $0.45 \text{ mg}\cdot\text{cm}^{-2}$ ) charged surfaces as compared to unpolarized ( $0.34 \text{ mg}\cdot\text{cm}^{-2}$ ) surface. This study indicates that protein adsorption is independent of charge polarity. However, a significant increase in cell density has been reported on the negatively polarized surface than positively polarized as well as unpolarized surfaces, while cultured with MC3T3 osteoblasts cells [70]. More recently, Yao et al. [182] investigated that polarized NKN shows significantly higher spreading and proliferation of rBMSCs cells as compared to unpolarized NKN. In another study, the addition (30 vol%) of polarized NKN with 1393 bioglass results in comparatively higher cell proliferation than monolithic 1393 bioglass [183].

Lithium modified NKN ( $\text{Li}_{0.06}\text{Na}_{5}\text{K}_{4.4}\text{NbO}_3$ , LNKN) ceramics possess excellent piezoelectric properties ( $d_{33} = 222$ ) [184], alongwith superior

biocompatibility as compared to unmodified NKN [75–77]. LNKN (polarized at ~ 22–24 kV/cm) exhibits excellent chemical stability and hydrophilicity against biological fluid, which indicates its suitability for orthopedic applications [75]. Electrically treated LNKN surface results in the rapid rate of apatite formation [77]. LNKN (polarized at E-field intensity of 22–24 kV/cm) supports 33% higher growth of osteoblasts on the polarized surface, as compared to that on the unpolarized surface [76].

The NKN has been potentially utilized to induce the piezoelectricity in HA-NKN functionally graded material (FGM) [178,185]. In FGM development, the piezoelectric NKN layer has been introduced between HA layers [185]. Such a concept of FGM development has been reported to increase the polarizability of HA by more than three times without affecting its excellent biocompatibility. However, the incorporation of the LNKN layer between HA layers increases the polarizability up to six times [178].

As discussed earlier, polarization plays a very important role in cellular functioning. The augmented polarizability of HA can potentially increase cellular growth and proliferation. The findings of above-mentioned studies are quite appealing in terms of augmented *in vitro* biocompatibility, which is attributed to the surface charge potential of the polarized piezoelectric NKN. Therefore, the clinical implications of polarized NKN-based ceramics can be realized as the physiological loads can generate surface electrical charge, which can stimulate bone regeneration [30,40]. Apart from the applications in bone tissue engineering, NKN-based ceramics can be utilized in nerve and skin replenishment as well as drug delivery [186].

#### 4.3.2. BaTiO<sub>3</sub>

BaTiO<sub>3</sub> exhibits phase transformation from symmetrical cubic (paraelectric or non-polar) to an asymmetric (ferroelectric or polar) structure below its Curie temperature (120 °C), which occurs due to the relative atomic displacements between the positive centroid Ti<sup>4+</sup> and face centered O<sup>2-</sup> ions [39]. Such kind of displacement develops spontaneous electrical polarization, even in the absence of electric field. The dipole moment changes its direction as a function of temperature, which

initiates further phase transformations. Such a phenomenon results in a net polarization which consequently, makes BaTiO<sub>3</sub> piezoelectric [5]. BaTiO<sub>3</sub> shows three ferroelectric phase transitions, from rhombohedral to orthorhombic to tetragonal, at temperatures of - 90 °C and 5 °C, respectively. Above 120 °C (T<sub>C</sub>), it transforms into a non-ferroelectric cubic phase.

Hwang et al. [39] performed *in vitro* bioactivity on BaTiO<sub>3</sub> ceramics, polarized above and below its Curie temperature (120 °C). The Ca/P ratio was recorded to be 1.5–1.7 on negatively charged BaTiO<sub>3</sub> surface, polarized above Curie temperature (160 °C, E<sub>p</sub> = 5 kV/cm). However, this ratio was 1.2–1.5 on the negatively charged surface, when polarized below Curie temperature at the same polarizing field [39]. A similar experiment has been performed by Park et al. [187] on BaTiO<sub>3</sub> ceramics, polarized above its Curie temperature (T = 160 °C, E<sub>p</sub> = 5 kV/cm). A thick layer of CaP has been observed on the negatively charged surface of the piezoelectric sample (see Fig. 3 (A)). Similarly, negatively charged BaTiO<sub>3</sub> thin film also has been demonstrated to enhance the cellular functionality of L929 mouse fibroblast cells than positively charged as well as uncharged films [188].

Park et al. [38] implanted unpolarized and polarized BaTiO<sub>3</sub> ceramics in canine femora of dogs for 16 and 86 days. The integration of an implant with the host bone tissue has been estimated in terms of output voltage (from the implant) in response to applied mechanical stimulation. As mentioned in Table 2, significantly high voltage output was observed for polarized implants, which suggests effective integration and consequently, the load transfer via the implant-tissue interface. The voltage output through the polarized implant was reported to be approximately proportional to the applied load, after 86 days of implantation. The increase in interfacial tensile strength indicates the strong mechanical bonding between bone and implant [Table 2] [72]. Therefore, polarized surface of BaTiO<sub>3</sub> implant shows good adaptability against surrounding tissues with a strong interfacial bonding.

Several studies revealed the potentiality of biocompatible HA-piezoelectric BaTiO<sub>3</sub> ceramic composites for the development of implant scaffolds [189–193]. It has been demonstrated that the proliferation of SaOS-2 cells on HA - (90 vol %) BaTiO<sub>3</sub> piezoelectric

**Table 2**  
*In vitro* and *in vivo* response of unpolarized and polarized BaTiO<sub>3</sub> ceramics.

S-N.	BaTiO <sub>3</sub> - based ceramics/ Composites	Fabrication/Processing route	<i>In vitro/in vivo</i> study	Key assessments	Ref.
1.	BaTiO <sub>3</sub>	Slip casting, followed by polarization (19 kV/cm)	Implantation in dog femur up to 12 weeks	Higher voltage output on polarized implant (0.95 mV) than unpolarized implant (0.08 mV) and natural bone (0.16 mV) indicating the maximum load transfer at polarized implant - host tissue interface	[38]
2.	BaTiO <sub>3</sub>	Slip casting, followed by polarization (19 kV/cm)	Implantation in dog femur for 20 weeks	Higher implant-tissue interfacial tensile strength (~2.3 MPa) after 3.5 weeks of implantation. Matured compact cortical bone after 95 days of implantation.	[72]
3.	BaTiO <sub>3</sub>	Solid state synthesis (CIP), polarized above and below Curie temperature at 5 kV/cm and 25 kV/cm, respectively	Bioactivity test for 30 days	Higher Ca/P ratio (1.5–1.7), as well as a thick layer of calcium phosphate, on the negatively polarized BaTiO <sub>3</sub>	[39]
4.	BaTiO <sub>3</sub>	Solid state synthesis (CIP), polarized above Curie temperature at 25 kV/cm	Bioactivity test for 30 days	A thick layer of CaP (0.8–0.9 μm) on the negatively charged surfaces	[187]
5.	HA- BaTiO <sub>3</sub>	Solid state synthesis (CIP), polarized (Polarization conditions not defined)	Implantation study of HA and HA - BaTiO <sub>3</sub> composite in the jawbones of dogs	Rapid rate of bone growth on HA - BaTiO <sub>3</sub> in a direction perpendicular to the polarization direction.	[189]
6.	HA - (90 vol %) BaTiO <sub>3</sub>	Solid state synthesis, followed by polarization at 4.54 kV/cm	Cell proliferation with SaOS-2 osteoblast-like cells	Cell growth enhancement (>13 times) after 7 days of culture	[190]
7.	HA - (90 wt %) BaTiO <sub>3</sub>	Slip casting, followed by polarization (8–14 kV/cm)	Cellular (osteoblasts) response and ALP activity under periodic loading	Increased cell viability and differentiation	[192]
8.	HA-coated porous BaTiO <sub>3</sub>	Sol-gel dip coating method	Bioactivity test up to 30 days	Bone-like apatite (CaP) layer on coated samples, after 30 days of soaking in SBF	[193]
9.	Polymer P(VDF - TrFE) - 10 vol % BaTiO <sub>3</sub> membrane	Film casting method	Human alveolar osteoblast cell, Implantation study in rabbit tibiae bone for 21 days	Augmented bone growth with high cell mitosis activity on BaTiO <sub>3</sub> - polymer composite surface as compared to monolithic polymer	[196, 197]
10.	Poly (Lactic-co-glycolic) acid or PLGA - (x wt. %) BaTiO <sub>3</sub> , x = 0, 10, 30	Porous composite scaffold prepared by solvent forming-salt leaching method	DNA concentration, cell differentiation study with M9C2 rat muscle cell	Almost double DNA concentration and high cell differentiation in polymer- BaTiO <sub>3</sub> composite scaffold	[73]

composite ( $d_{33} = 57.8 \text{ pC/N}$ ) increases by 12 times after 7 days of culture as compared to those cultured for one day [190]. On the other hand, under physiological loadings (0–100 N, frequency = 0–5 Hz), polarized HA - 90 wt % BaTiO<sub>3</sub> surface enhances osteoblastic cell proliferation and differentiation than HA [192]. In HA - BaTiO<sub>3</sub> composite, the global piezoelectric properties depend upon the fraction of the BaTiO<sub>3</sub> phase. For example, HA - (70–75 vol %) BaTiO<sub>3</sub> composites possess  $d_{33}$  value of less than unity (pC/N), which increases to 18 pC/N for HA-80 vol % BaTiO<sub>3</sub> composite [194]. However, the composites with less than 70 vol % BaTiO<sub>3</sub> do not exhibit piezoelectricity and the ferroelectric domains exist only for composites with quite high ( $\geq 95\%$ ) content of BaTiO<sub>3</sub> [194]. However, poling treatment of HA-BaTiO<sub>3</sub> composite has been revealed to induce the cellular response.

In order to substantiate this aspect, Fig. 5 (A and B) illustrates that the osteoblasts growth, while cultured on uncharged and charged HA-20/40 wt % BaTiO<sub>3</sub> composites, is modulated as a function of the addition of piezoelectric secondary phases to HA matrix [17]. In case of HA-20 wt% BaTiO<sub>3</sub>, the effect of surface charges is not observed as the

cell growth on uncharged and charged samples are almost similar. This is due to lower content (20 wt%) of piezoelectric BaTiO<sub>3</sub> phase. However, the effect of surface charges is clearly observed for higher content (40 wt%) of piezoelectric phase, where significantly higher cell growth is observed for negatively charged surfaces as compared to positively charged or uncharged surfaces [17]. Fig. 5 (C) schematically demonstrates that higher content of piezoelectric phase generates more amount of electrostatic charge, which consequently, stimulates the cellular response [17]. The anticipated toxicity concern of BaTiO<sub>3</sub> particulates has been addressed by intra-articular injection of HA-40 wt% BaTiO<sub>3</sub> particles (up to 25 mg/ml) in the knee joint of mice (Fig. 5 (D) [195]. The activity and weight of mice were observed to be normal up to 7 days of post-injection. Histopathological analyses suggest that the injected particles were neither translocated to any of the major organs such as heart, kidney, liver, lung etc. nor caused any adverse effect to these organs [195]. These results confirm the absence of any systemic toxicity of such piezo-biocomposites. It has been demonstrated that the injected particles were accumulated in the close vicinity of knee joint region

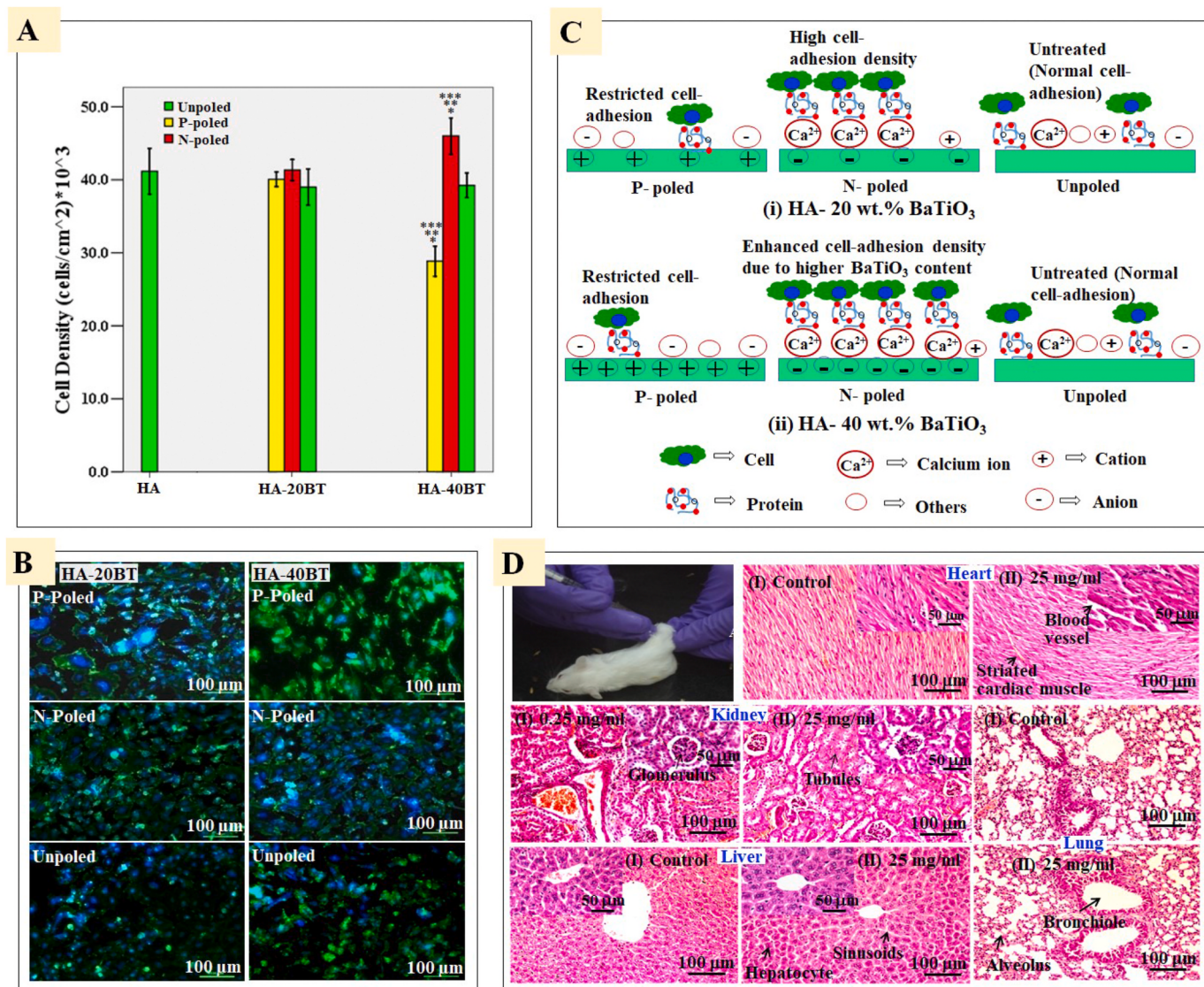


**Fig. 5. Surface charge induced biocompatibility of HA-BaTiO<sub>3</sub> composites.** (A) & (B) Quantitative and qualitative assessments of cell response on uncharged and negatively as well as positively charged HA-20 wt% BaTiO<sub>3</sub> (HA-20 BT) and HA-40 wt% BaTiO<sub>3</sub> (HA-40 BT) composites (Reproduced with the permission from the publisher, Ref. [17]). (C) Mechanistic description of the surface charge induced cell growth on HA-20 B T and HA-40 B T composites (Reproduced with the permission from the publisher, Ref. [17]). (D) Intra-articularly injected HA-40 wt% BaTiO<sub>3</sub> particulate in the knee joint of mice could not cause any systematic toxicity in vital organs, such as heart, kidney, liver and lung at 7 days of post-injection, as evident from representative fluorescent images (Reproduced with the permission from the publisher, Ref. [195]).

without causing any inflammatory/foreign body reaction [195]. Therefore, the potentiality of HA-BaTiO<sub>3</sub> composite as prospective prosthetic implant can be realized.

The above discussion suggests that the stress generated electrical potential, due to piezoelectricity, promote osteogenesis. The idea behind the application of such a dynamic loading condition was based on the fact that natural bone undergoes various loading conditions during our daily life activities. Jianqing et al. [189] fabricated HA-BaTiO<sub>3</sub> composite and polarized in the direction of its longitudinal axis. Thereafter, these composites were implanted vertically and horizontally in the jawbones of dogs. It has been observed that the surface of the vertically implanted specimen develops more neobone as compared to that of the parallelly implanted specimen. It indicates that osteogenesis is direction-dependent and promoted in the direction of polarization (i.e. longitudinal axis of the specimen). In addition, the rate of tissue formation has been observed to be higher on HA - BaTiO<sub>3</sub> composite than the control (HA) sample.

Several studies reported the piezoelectric BaTiO<sub>3</sub> induced improved biocompatibility in polymers where the combined effect of physicochemical properties of both piezoelectric BaTiO<sub>3</sub> ceramic and polymer play a crucial role in promoting osteogenesis, *in vitro* as well as *in vivo* [73,196,197]. Beloti et al. [197] observed augmented cellular response on the piezoelectric polymer membrane [p(VDF-TrFE) - BaTiO<sub>3</sub>] as compared to non-piezoelectric polymeric (e-polytetrafluoroethylene or e-PTFE, used as control) membrane, when cultured with human osteoblast cells. Such kind of increased cellular proliferation/differentiation takes place as a consequence of excellent wettability as well as protein binding ability of piezoelectric p(VDF-TrFE) - BaTiO<sub>3</sub> membrane in culture medium. The porous composite scaffold prepared by the incorporation of 30 wt % of piezoelectric BaTiO<sub>3</sub> nanoparticles in poly (Lactic-co-glycolic) acid or PLGA polymer matrix has been reported to double the cellular DNA content and significantly increases the myotube dimension (length: from 60 to 100 μm, width: from 9 to 14 μm) than those on pure PLGA polymer, when cultured with H9C2 (rat myoblast) cells for 3 days [73].

Gimenes et al. [196] demonstrated the augmented bone growth, when the thermally treated (1200 °C for 4 h) thin film of poly (vinylene - trifluoroethylene) [P(VDF-TrFE)] - 10 vol % BaTiO<sub>3</sub> piezoelectric composite membranes were implanted into male rabbit tibiae for 21 days. The neobone formation has been triggered by electrical stimulation produced from the strained piezoelectric membrane during physical activity of rat. Li et al. [198] reported that the biocompatibility as well as mechanical compatibility of nano-sized titania ceramics can be improved by the addition of piezoelectric BaTiO<sub>3</sub> nanoparticles. The inherent piezoelectricity of BaTiO<sub>3</sub> nanoparticles enhances the biological response of nano titania composite.

**Table 2** summarizes *in vitro/in vivo* response of piezoelectric BaTiO<sub>3</sub> ceramic-based materials for orthopedic implant applications [38,39,72, 73,187,189,190,192,193,196,197]. From the above discussion, it can be concluded that the piezoelectric potential of BaTiO<sub>3</sub> in monolithic/composite form stimulates apatite formation, cellular functionality as well as hard tissue regeneration. The excellent short-term and long-term biocompatibility in small and large animal models suggests its capability for the clinical trials.

#### 4.3.3. MgSiO<sub>3</sub>

MgSiO<sub>3</sub> (MS) possesses an asymmetric tetragonal perovskite structure, which is responsible for its piezoelectricity and spontaneous polarization [103]. The biodegradable nature of MgSiO<sub>3</sub> facilitates the piezoelectric implant to be easily replaced by newly developed bone tissue [144].

A porous scaffold consisting of HA nanowire - MgSiO<sub>3</sub> nanocomposite with Chitosan polymer i.e., HA-MS-CS [(HA-MS): CS = 7 : 3 wt ratio] demonstrates enhanced rat bone marrow mesenchymal stem cells (BMSC) [143]. In addition, *in vivo* dissolution study shows augmented bone formation on HA-MS-CS scaffold, after 12 weeks of

implantation in the scalp and calvarium of rats, as compared to control scaffolds, i.e., without MgSiO<sub>3</sub> [Fig. 6] [143]. Such kind of promoted osteogenesis has been suggested to occur due to the excellent biodegradability of MgSiO<sub>3</sub>. MgSiO<sub>3</sub>-based polymer (HA-MS-CS) composite releases Mg<sup>2+</sup> and Si<sup>4+</sup> ions that differentiate the rat bone marrow mesenchymal stem cells or rBMSC into osteoblast cells. Such osteogenic differentiation results in enhanced bone regeneration after 12 weeks of implantation [Fig. 6 (A)] [143]. Percentage of neobone area and bone volume in (HA-MS-CS) implant were increased by (1.71, 1.6 times) than HA-CS and (12.5, 8.16 times) than CS scaffold [Fig. 6(B) and (C)] [143]. In addition, other factors such as osseointegration, angiogenesis also increase in MgSiO<sub>3</sub>-based polymer composite [143]. Overall, MgSiO<sub>3</sub> induces the osteogenic performance of the composite.

The composite scaffold of MgSiO<sub>3</sub> with various polymers, such as, poly (butylene succinate) or PBSu (solvent forming - particulate leaching method), Chitosan polymer, poly (ε-caprolactone) or PCL (solvent forming - particulate leaching or rapid prototyping method), poly (ethylene glycol) or PEG (solvent forming - particulate leaching method), and wheat protein or WP (natural polymer) (sol-gel - compression molding method) have been reported to improve the osteogenic performance [81,82,144,199,200]. A scaffold comprising of amorphous *m*-MgSiO<sub>3</sub>, polycaprolactone (synthetic polymer) and wheat protein (natural polymer) show augmented *in vitro* biodegradability, biominerilization, and osteogenesis [82]. Such behaviors are the consequences of favorable biodegradability and hydrophilicity of composite scaffolds.

Although, biodegradability facilitates cell growth and bone regeneration with MgSiO<sub>3</sub> based scaffolds, the uncontrolled biodegradability limits their *in vivo* trials up to small animal models. Therefore, standardized fabrication methods are to be developed to control the biodegradability of such scaffolds before their implantation in large animal models and subsequent, clinical trials. **Table 3** briefly summarizes *in vitro* and *in vivo* response of MgSiO<sub>3</sub>-based ceramics, reflecting on the improved osteogenic performance [80–82,143,144,199,200].

#### 4.3.4. LiNbO<sub>3</sub>

LiNbO<sub>3</sub> is a well-known ferroelectric material with excellent polarizability (spontaneous polarization,  $P_s = 78 \mu\text{C}/\text{cm}^2$ ) [145] at room temperature, which can be easily reversed by the application of the electric field. Apart from stable polarizability, LiNbO<sub>3</sub> also possesses good pyroelectric ( $P_r = 103.9 \mu\text{C}/\text{m}^2\text{K}$ ) [101] as well as piezoelectric properties ( $d_{33} = 23 \text{ pC/N}$ ) [79]. The electroactive LiNbO<sub>3</sub> surface adsorbs the organic molecules, like D-cysteine, which helps in stimulating polarized LiNbO<sub>3</sub> surface for protein adsorption [201].

Carville et al. [78] demonstrated that the charged surfaces of LiNbO<sub>3</sub> induces ions exchange and protein interaction from cell media which consequently, results in significant enhancement in the proliferation of MC3T3 osteoblast cells, irrespective of charge polarity. In another study, it has been reported that the negatively charged surfaces facilitate significant cellular (NIH-3T3) elongation with more spreaded cell morphology as compared to the positively charged surfaces [145]. The negatively polarized LiNbO<sub>3</sub> surface promotes the adhesion of cations, which further attracts electronegatively charged cellular membrane. However, positively charged surface attracts negatively charged ions, which restricts the adhesion of cells and in fact causes cell migration [145]. In contrast, positively charged surface of LiNbO<sub>3</sub> exhibits 15% higher wound healing (cellular migration) capability than the negatively charged surface, which was almost double than that of the glass control surface [145].

On the other hand, Vanek et al. [79] elucidated a different hypothesis that the positively charged surface of polarized LiNbO<sub>3</sub> substrate preferably adsorbs electronegatively charged cell-adhesion proteins such as fibronectin and vitronectin. Therefore, the cell differentiation is promoted on the positively charged surface (0.037 ALP/μg of BCA protein) as compared to the negatively charged surface (0.030 ALP/μg of BCA protein) of LiNbO<sub>3</sub> [79]. Overall, these results indicated that

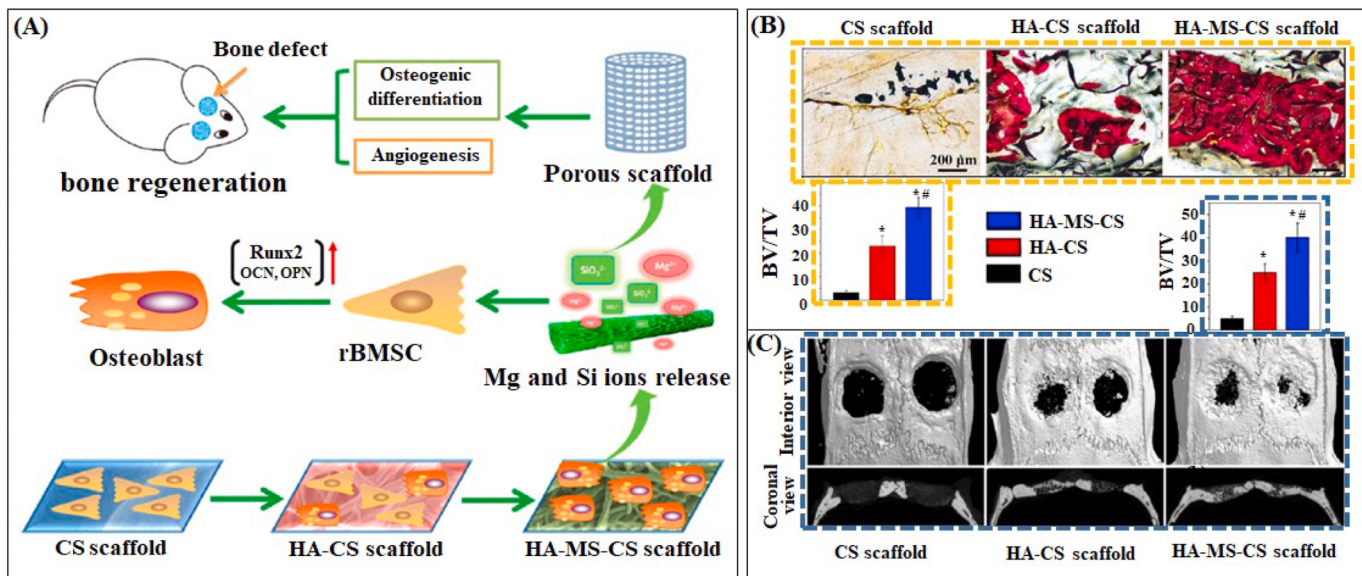


**Fig. 6.** Hypothesis of osteogenic differentiation of rat bone marrow mesenchymal stem cells (rBMSCs) into osteoblasts cells, recruited in bone healing [(A) and (B)]. (A) Due to biodegradable nature of  $\text{MgSiO}_3$  (MS), the  $\text{Mg}^{2+}$  and  $\text{Si}^{4+}$  ions degrade from the  $\text{MgSiO}_3$ -based polymeric scaffold, which accelerates the differentiation of rBMSCs into osteoblasts cells and results in bone regeneration, when implanted in the defected site of rat calvaria; (B) Histological evidences of bone regeneration at the defected region with CS, HA-CS and HA-MS-CS implant, where red stains indicate newly formed bone. HA-MS-CS scaffold shows higher amount of newly developed hard tissues as compared to HA-CS and CS scaffold (see quantitative plot of BV/TV, BV: bone volume and TV: total volume); (C) Micro-CT image of bone growth at the defect region, where piezoelectric MS based scaffold (HA-CS-MS) and control scaffold without MS (i.e., CS, HA-CS) were implanted for 12 weeks. Coronal and interior 3-D view demonstrated augmented bone growth with implantation of piezoelectric MS aided (HA-CS-MS) scaffold, both qualitatively and quantitatively (Reproduced with the permission from the publisher, Ref. [143]). (For interpretation of the references to colour in this figure legend, the reader is referred to the Web version of this article.)

**Table 3**  
Summary of biocompatibility studies on  $\text{MgSiO}_3$  (MS) ceramics.

S-N.	MgSiO <sub>3</sub> -based ceramics/Composite	Fabrication/Processing route	In vitro/in vivo study	Key assessments	Ref.
1.	Mesoporous $\text{MgSiO}_3$ (m- MS)	Precipitation -centrifugation method	Biomineralization, osteoblast cell proliferation and ALP activity with MC3T3-E1 osteoblast cells; biodegradability study	The rapid rate of apatite formation, enhanced cell proliferation, and ALP activity after 7 days of seeding	[80]
2.	HA Nanowire - nanosheet $\text{MgSiO}_3$ - Chitosan polymer (HA-MS-CS polymer)	Porous scaffold prepared through the solvothermal method	Cytocompatibility with rat bone marrow mesenchymal stem cells or rBMSCs, 12 weeks implantation in rat bone	Neobone formation, higher blood vessel number around HA-MS-CS scaffold ( $40.15 \pm 6.11\%$ ; $50 \pm 7$ ) than HA-CS ( $25.06 \pm 3.74\%$ ; $29 \pm 8$ ) and CS scaffold ( $4.92 \pm 1.24\%$ ; $13 \pm 5$ ).	[143]
3.	X (m-MS) -Poly (Butylene succinate) polymer composite, X = 20, 40 wt %	Solvent forming-particulate leaching method	Cellular response and ALP activity with MC3T3-E1 osteoblast cells, <i>In vitro</i> bioactivity, Implantation in rabbit femur	Highest cell viability and cell differentiation on m-MS (40 wt %)-based composite after 5 days; Maximum bone growth observed in [(40 wt %) m-MS - polymer] composite	[81]
4.	m-MS(30 wt %) - (PCL-PEG-PCL) polymer composite	Solvent forming-particulate leaching method	Cellular response and ALP activity with MG-63 (human osteosarcoma) cells; Implantation in the rat femur bone	Faster cell differentiation observed in m-MS-based polymer composite, 1.5 times higher newly formed bone in mMS-based polymer composite than without m-MS-based composite	[199]
5.	X (m-MS) -poly (ε caprolactone) - poly(ε ethylene glycol)-poly(ε caprolactone), X = 0, 20, 40 wt %	Solvent forming-particulate leaching method	Hydrophilicity, bioactivity, cell and ALP activity with MG-63 cells	Uniform dense apatite layer, highest cell adhesion, and proliferation observed in 40 wt % m-MS polymer composite than composite with lower or non-MS	[200]
6.	Amorphous Xm-MS-wheat protein polymer composite, X = 0, 20, 40 wt %	Sol-gel- compression molding method	Bioactivity, cell and ALP activity with MC3T3 osteoblast cells	Cell viability and cellular differentiation increased with the increase in MS fraction in polymer scaffold	[144]
7.	Amorphous m-MS-PCL-WP	Rapid prototyping approach	Bioactivity, hydrophilicity, cytotoxicity test (L929 cells), hMSCs cell proliferation and differentiation (ALP test).	Increased cell proliferation and differentiation after 14 days	[82]

ferroelectric  $\text{LiNbO}_3$  ceramics exhibit excellent spontaneous polarization which facilitates cell proliferation/differentiation. Therefore, this piezoelectric ceramic can be utilized as a prospective implant where one's physiological activity generates sustainable charge at the defect site to stimulate osteogenesis. However, long term *in vivo* biocompatibility has to be investigated.

#### 4.3.5. $\text{KNbO}_3$

$\text{KNbO}_3$  is an emerging piezoelectric perovskite material having its application in the biomedical field as a bio-probe for disease diagnosis [83,146,147].  $\text{KNbO}_3$  nanowires also find their application in scanning light imaging in life sciences, due to their second harmonic generation with larger non-linear stable polarizability, at room temperature. Therefore, it has the ability to be used as a tunable coherent light source

[146]. KNbO<sub>3</sub> nanocrystals, coated with amino dextrin (AD), have been demonstrated as a bio-marker for the diagnosis of non-tumor cells, as AD coated KNbO<sub>3</sub> nano-crystals suitably attach with the human lung derived BEAS-2B non-tumor cells [147]. In addition, KNbO<sub>3</sub> nanoparticles are suggested to be highly toxic for prostate cancerous cells (DU-145), which enables the application of KNbO<sub>3</sub> in prostate cancer treatment [83].

#### 4.3.6. ZnO

Zinc has been proved as an important element that stimulates the osteoblastic activities [202]. ZnO is available in three different crystal forms, namely, zinc blends, rock salt, and wurtzite. Among which, wurtzite possesses a tetrahedral non-centrosymmetric structure and therefore, exhibits piezoelectricity [203].

Owing to its piezoelectric nature, nanosized ZnO sheets develop a local electric field in response of inherent mechanical force from the cells, which improves the metabolic activity of human SaOS-2 osteoblast-like cells and macrophages [44]. The growth of cells on the piezoelectric ZnO nanosheets occur through the activation of different types of calcium channels such as, voltage-gated Ca<sup>2+</sup> channels (VGCC), stretch activated Ca<sup>2+</sup> channels (SACC) and membrane receptors [44]. Due to the inherent stress from cells on the piezoelectric nanosheets and locally developed electrical charges, the membrane potential of adjacent cell changes. Consequently, voltage-gated Ca<sup>2+</sup> channels and stretch activated Ca<sup>2+</sup> channels open, which allows the influx of extracellular Ca<sup>2+</sup> ions [44]. The local electrical field can modify the configuration of membrane receptors and opens receptor channels, which allow an influx of intracellular Ca<sup>2+</sup> ions from the endoplasmic reticulum [44]. Consequently, intracellular Ca<sup>2+</sup> ions increase and this stimulates the growth of cells on the piezoelectric ZnO nanosheets.

Foroutan et al. [204] suggested that for a particular fixed nanosize, biological activities of bone marrow mesenchymal stem cells (BMSC) reduce at higher concentration (60 µg/ml) of ZnO nanoparticles as compared to lower concentration (30 µg/ml), which indicates the concentration dependent cytotoxicity of ZnO. Apart from concentration, cytotoxicity of ZnO also depends on particle size and pore density [205, 206]. The cytotoxicity of ZnO increases with the reduction in particle size to the nanoscale level due to the generation of reactive oxygen species (ROS) [205]. In addition, the functionality of fibroblast cells improves with an increase in pore density due to the large reactive surface area for proteins as well as cell adhesion [206]. In contrast to the above discussion, ZnO nanorods show the toxic behavior against macrophages as compared to their flat surfaces and therefore, ZnO nanorods reduce macrophages associated inflammatory response [207].

There are number of literature reports which suggest that an optimized amount of ZnO reinforcement to a biomaterial causes a reasonable increase in the compatibility with fibroblasts, osteoblasts, stem cells, etc. [208–210]. For example, Dikici et al. [208] reported a continuous increase in cell density of hMSCs with increasing the content of ZnO up to 0.5 wt % in calcium sulphate-based scaffold. It has been suggested that the improved cellular response is observed due to piezoelectric ZnO induced hydrophilicity [208]. The osteogenic response of polymeric scaffolds, such as PCL and polyurethane, can be improved with the addition of an optimal amount of piezoelectric ZnO [209,210]. Shrestha et al. [209] observed the stimulated osteogenic proliferation and differentiation of pre-osteoblast MC3T3-E1 cells on polyurethane-based polymer scaffold by introducing ZnO (0.2 wt %) nanoparticles. A nanofibrous scaffold, prepared by incorporating 1 wt % of ZnO in PCL-HA has been reported to be more osteoactive against human fetal osteoblast (hFOB) cells as compared to scaffolds without ZnO [210]. In addition to piezoelectricity, the improved biological response of ceramic matrix was attributed to the sustainable release of zinc ions which regulates various cell metabolic activities such as protein synthesis, mRNA expression etc. [211,212]. From the above discussion, it can be commented that long term *in vivo* experiments with small and large animal models are required prior to it's realistic clinical

applications.

#### 4.3.7. Boron nitride

Boron, even at the molecular level, plays an important role in modulating the osteoblastic functionality of MC3T3-E1 [213] and hMSC [214] cells by regulating the level of bone morphogenetic proteins (BMP), osteocalcin, RunX2 (transcription factor), mRNA expression etc. These factors play an important role in regulating osteogenic metabolism [215, 216, 217]. For example, Nakhmanson et al. [218] investigated the piezoelectricity and spontaneous polarization in boron nitride nanotubes (BNNT). BNNT supports the differentiation of hMSCs into osteoblast cells by releasing a trace amount of boron in culture medium and the stress applied from BNNT fibers on the hMSC cells [84]. Such kind of stress causes stretching of cells that activate actin filament and consequently, results in enhanced osteogenesis [84]. Another factor, which promotes the osteogenesis of BNNT is their positive affinity for cellular protein [219]. The adherence and proliferation of MG-63 and hMSCs are enhanced on Ackermans - BN composite scaffold [220]. The electrospun mats, prepared by the reinforcement of 1–5 wt % boron nitride on gelatin polymer, exhibit good biomaterialization and cytocompatibility with HOS human osteosarcoma cells [221]. A balanced reinforcement of hexagonal BN (0.3–0.5 wt %) with PCL-TCP also facilitates the successful proliferation of human osteoblast-like SaOS-2 cells [222]. Overall, the above mentioned literature reports clearly suggest the potentiality of boron nitride for bone tissue engineering applications.

#### 4.3.8. Piezoelectric polymers

The inherent piezoelectricity and biocompatibility of a specific class of polymers make them suitable for bone tissue engineering applications. These polymers can be classified as synthetic and natural piezoelectric polymers. The synthetic piezoelectric biocompatible polymers include  $\beta$ ,  $\gamma$  or  $\delta$  phases of polyvinylidene fluoride (PVDF) and its copolymer, poly-L-lactic acid (PLLA), polyhydroxybutyrate (PHB) and polyamides (Nylons, peptides, etc.), etc. Some of the biocompatible polysaccharides such as, cellulose (wood, ramie), chitosan, amylose (starch), and proteins such as, collagen, silk, keratin possess inherent piezoelectricity, which are categorized as natural piezoelectric polymers. A number of methods are available to fabricate piezoelectric polymer-based scaffolds for bone tissue engineering applications, such as, compression molding, solvent casting and particulate leaching, phase separation method, gel casting, solid free form, gas foaming, fiber electrospinning, rapid prototyping, fused deposition, three-dimensional printing and selective laser sintering [223–226].

**4.3.8.1. Synthetic polymers.** The piezoelectricity has been observed in the stretched and polarized film of PVDF polymer [227]. The semi-crystalline PVDF polymers consist of five phases ( $\alpha$ ,  $\beta$ ,  $\gamma$ ,  $\delta$  and  $\varepsilon$ ). Amongst these polymorphs,  $\beta$ ,  $\gamma$ , and  $\delta$  phases possess permanent dipole moment and exhibit piezoelectricity [113]. It has been reported that the non-piezoelectric  $\alpha$  phase of PVDF can be changed into the piezoelectric  $\beta$  phase through stretching and poling [228]. Electrospinning is a quite appealing fabrication technique for the production of piezoelectric phased polymers [229,230]. The biocompatibility of piezoelectric PVDF polymeric substrates has been investigated with MC3T3-E1 osteoblast cells [29,225,231–233], human mesenchymal stem cell (hMSCs) [229, 234], human adipose stem cells (hASC) [235,236], and goat marrow stem cells [237]. Polarized PVDF film induces protein adsorption and subsequent, increase in pre-osteoblast cell density, where electroactive film generates sufficient electrical potentials [231–233]. Apart from film, PVDF microparticles provide a feasible environment for the growth of MC3T3-E1 osteoblast cells [225]. Damaraju et al. [229] reported that electrospun (@ 25 kV) PVDF fibers enhance the osteogenic differentiation of human mesenchymal stem cells (hMSC) into osteoblast cells and early matrix mineralization as compared to electrospun fibers (@12 kV).

It has been suggested that the augmented osteogenic response is attributed to the higher piezoelectric  $\beta$  phase (72%), electrospun at 25 kV. However,  $\beta$  phase content was 67% in the PVDF fibers, electrospun at lower potential. PVDF microparticles promote the viability and differentiation of hMSC [234]. Similarly, piezoelectric PVDF film also promotes the differentiation of human adipose stem cells, where polarized surfaces are found to be hydrophilic [235]. In another study, it has been demonstrated that piezoelectric PVDF exhibits significantly increased adhesion and proliferation of goat bone marrow stromal cells

under dynamic culture. In addition, such a piezoelectric film supports the differentiation of goat marrow stromal cells into osteoblast cells [237].

In the context of pre-clincial validation, Marino et al. [41] reported significantly increased osteogenic performance on polarized PVDF as compared to an unpolarized polymer substrate, when implanted in the interosseous membrane of rat tibia for six weeks. It has been suggested that bone growth is attributed to the piezoelectric signals, generated by the polarized surfaces. The polarized piezoelectric PVDF films and fibers

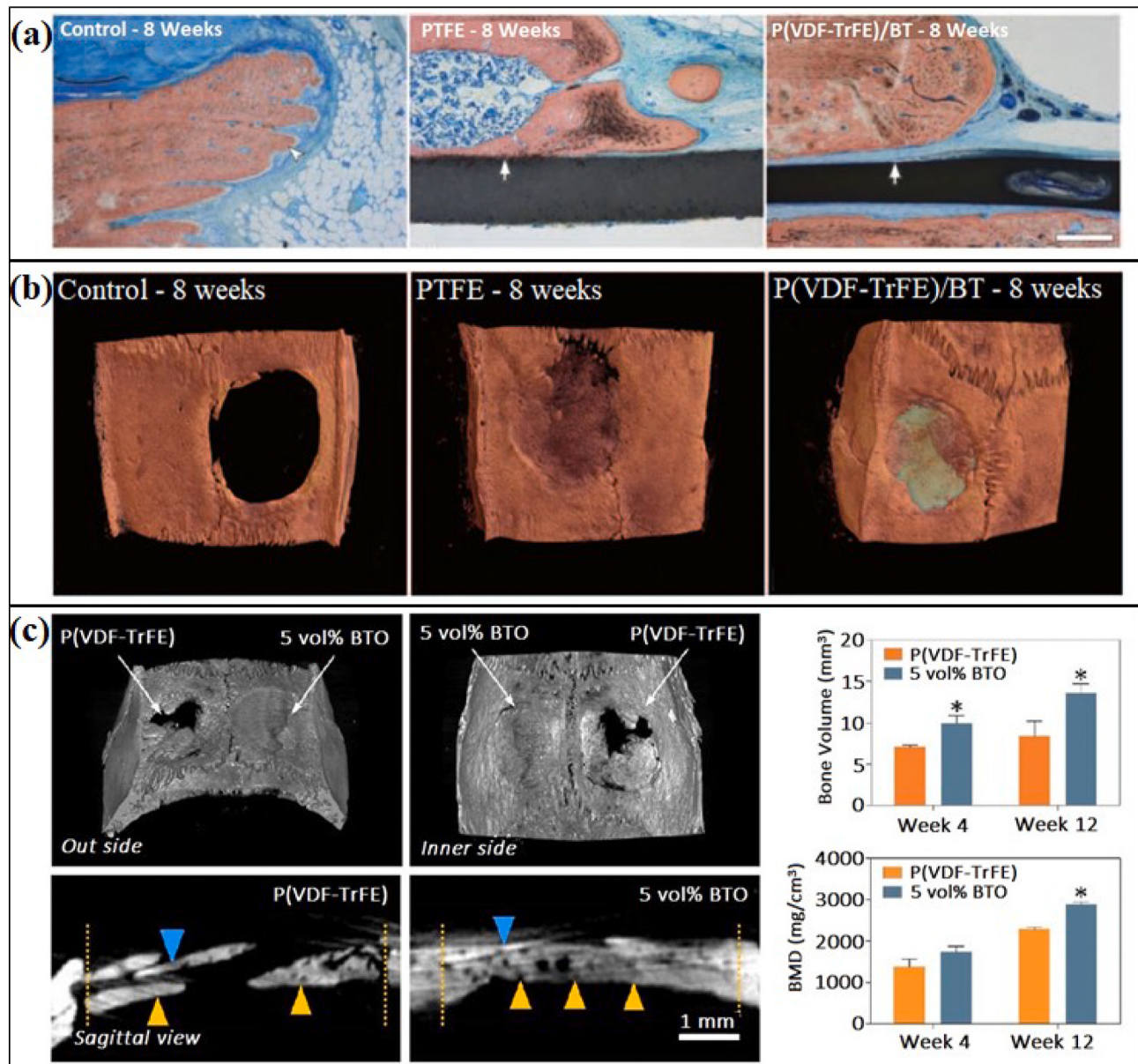


**Fig. 7. P(VDF-TrFE)/BT induced calvarial bone defect repair in rat.** Histology and micro-CT 3D images demonstrating the connective tissue formation on the calvarial bone defect of rat, while implanted with P(VDF-TrFE)/BT, polytetrafluoroethylene (PTFE) and control for 8 weeks [(a) and (b)] (Reproduced with the permission from the publisher, Ref. [243]). (a) The interface between P(VDF-TrFE)/BT and bone tissue is filled with a layer of newly developed tissue (white arrow), which was absent between PTFE implant and empty defect. (b) Newly developed bone tissue can be visualized on piezoelectric P(VDF-TrFE)/BT and PTFE. (c) Micro-CT images representing the bone defect repair of rat calvarial bone after 12 weeks of implantation with P(VDF-TrFE) – 5 vol% BaTiO<sub>3</sub> (BTO) membrane and neat P(VDF-TrFE) membrane. Blue arrow: membrane material, yellow arrow: newly developed hard tissues, yellow dotted lines differentiate the host bone from newly generated bone (Reproduced with the permission from the publisher, Ref. [28]). The rat calvarial defect implanted with P(VDF-TrFE) – 5 vol% BTO, completely covered with newly developed bone tissues; however, neat P(VDF-TrFE) implanted region shows comparatively lower tissue reparation. Sagittal view of micro-CT analyses further corroborated that P(VDF-TrFE) – 5 vol% BTO implanted membrane demonstrated comparatively higher bone tissue regeneration as compared to P(VDF-TrFE) implanted membrane. P(VDF-TrFE) – 5 vol% BTO implanted membrane induces significantly higher bone volume and bone mineral density as compared to neat P(VDF-TrFE) membrane after 12 weeks of implantation. BMD: Bone mineral density. (For interpretation of the references to colour in this figure legend, the reader is referred to the Web version of this article.)

facilitate increased bone regeneration as compared to unpolarized PVDF, in rat's femur [42].

PVDF polymer can also be used to develop piezoelectric actuator devices for implantation which has been demonstrated to stimulate hard tissue growth at the implant-tissue interface [231,238]. Owing to the inverse piezoelectric effect, the piezoelectric actuator generates mechanical stimulation at the interface which subsequently, assists in bone regeneration at the implanted region [231,238]. However, poor biodegradability of PVDF restricts their clinical applications and therefore, suitable fabrication technique or chemical/surface modification needs to be adapted to control it's degradability.

Recently, Kitsara et al. [239] treated the surface of the electrospun PVDF 3D scaffold with oxygen plasma to augment the cellular response. It has been demonstrated that SaOS-2 cell viability increases due to an increase in hydrophilicity (contact angle reduces from 130° to 35°) of oxygen plasma treated samples. The copolymers of PVDF, such as P(VDF-TrFE) ( $d_{33} = -38 \text{ pC/N}$ ) also reported as a potential piezoelectric substitute for hard tissue engineering applications [120, 240]. Damaraju et al. [240] fabricated a 3D scaffold of P(VDF-TrFE) polymer via electrospinning technique and examined hMSC response under dynamic conditions. It has been demonstrated that the combined action of piezoelectricity and mechanical stimulation results in higher proliferation, differentiation, extracellular matrix mineralization and gene expression, as compared to the mechanically stimulated non-piezoelectric scaffold. P(VDF-TrFE) tube shaped polarized scaffold has been suggested to promote the fibrous tissue growth on the negatively charged inner surface, when implanted in mice's femur [241]. The implantation of PVDF - starch and P(VDF-TrFE) - starch in rabbit femur results in the formation of a large number of macrophages as well as giant cells at the implanted region, which indicates an excellent foreign body response [242]. In addition, the value of the elastic modulus of implanted blends was found to be similar to that of the cancellous bone. The addition of piezoelectric BaTiO<sub>3</sub> in piezoelectric P(VDF-TrFE) has been observed to further improve the metabolic activity of hMSC cells and stimulate neo-bone formation [28,243].

Lopes et al. [243] compared the P(VDF-TrFE) – 10 vol% BaTiO<sub>3</sub> piezoelectric composite, and polytetrafluoroethylene (PTFE) to assess neo-bone formation by the implantation in rat calvarial defect for 4 and 8 weeks, respectively. It has been suggested that piezoelectricity and hydrophilicity in P(VDF-TrFE) – BaTiO<sub>3</sub> composite enhances their protein binding affinity, which further results in augmented osteogenesis. Light microscopy and micro-CT images [Fig. 7(A) and (B)] revealed that P(VDF-TrFE) – 10 vol % BaTiO<sub>3</sub> and PTFE implant shows remarkable hard tissue growth as well as connective tissue formation at the interface of implanted piezoelectric membrane [243]. In addition, significantly increased bone surface and lower trabecular separation was reported on piezoelectric P(VDF-TrFE) – 10 vol % BaTiO<sub>3</sub> composite as compared to PTFE, which clearly indicates the bone growth potential of the piezoelectric substrate. In a similar study, it was observed that the addition of 5 vol % polarized BaTiO<sub>3</sub> nanoparticles further enhances the bone tissue formation on P(VDF-TrFE) membrane [Fig. 7 (C)] [28].

P(VDF-TrFE) – 5 vol% BaTiO<sub>3</sub> piezoelectric membrane implanted in rat calvarial bone defect generates electrical microenvironment in response to the physiological loads which remains conserve during implantation period. Therefore, polarized BaTiO<sub>3</sub> nanoparticles added P(VDF-TrFE) membrane shows significant increase in newly formed bone volume and bone mineral density (BMD) as compared to neat P(VDF-TrFE). It has been demonstrated that the boron nitride nanotube or BNNT addition increases the piezoelectric property of P(VDF-TrFE) polymer by almost 2 times which results in increased osteogenic differentiation on P(VDF-TrFE) - BNNT composite as compared to P(VDF-TrFE) polymer [244].

Poly (L-Lactic) acid or PLLA is another synthetic polymer with reasonable piezoelectricity ( $d_{14} = -10 \text{ pC/N}$ ) and biodegradability [133,245]. Barroca et al. [246] demonstrated the surface polarization induced fibronectin adsorption on PLLA film, prepared by spin coating.

The *in vivo* assessment on piezoelectric PLLA substrates, in the form of film and rod, corroborate the suitability of this polymer as a potential alternative for hard tissues [Table 4] [247,248]. The physiological load applied on the piezoelectric implant generates electrical stimuli, which results in the rapid rate of bone regeneration at the defect region. The bone mimicking scaffold of PLLA with apatite and collagen generates bone-like environment in the extracellular medium, which stimulates the metabolic activities of SaOS-2 and hFOB cells [249,250]. Ko et al. [251] prepared a nanofiber composite scaffold of PLLA and nano-sized demineralized bone powder (DBP) via electrospinning method and studied their biocompatibility *in vitro* and *in vivo*. It has been observed that PLLA - DBP nanofiber composite scaffold effectively promotes the osteogenic differentiation of hMSC cells and efficiently healed the skull defect in the rat model. The degradability of PLLA limits their processability which can be overcome by starch blending. Starch increases ductility and compression modulus of PLLA and consequently, improves the processability [252]. PLLA is currently being used to make fastening devices for orthopedic application such as bone plate, screws, pins, washers etc. due to its excellent ossointegration [253,254].

The piezoelectric poly 3-hydroxybutyrate or PHB ( $d_{14} = 1.3 \text{ pC/N}$ ) is a member of a polyester polyhydroxyalkanoates (PHA), which has been demonstrated to be biodegradable [255–257]. Several studies have been performed with PHB and its copolymers such as, PHBHV or poly(3-hydroxybutyrate-co-3-hydroxyvalerate) and PHBHH or poly(-hydroxybutyrate-co-hydroxyhexanoate)-based polymers to investigate their biocompatibility, *in vitro* [87,258–263] and *in vivo* [264–266] (Table 4). The poor mechanical properties of PHB polymer limits their load bearing clinical applications however, it can be improved by the blending with other polymers such as PHBHH, PCL etc. [267,268].

Polymers with odd numbered amide-like CONH bonds (nylon, polypeptides, etc.) also possess piezoelectricity, mainly due to internal rotation of CO and NH dipoles and the presence of asymmetric carbon atom [257, 269]. The results of a number of studies demonstrate the potential application of piezoelectric polyamides-based scaffolds for bone tissue engineering applications [Table 4] [88,270–275].

**4.3.8.2. Natural polymers.** Natural polymers can be classified into two main groups, proteins, and polysaccharides. Proteins, which exhibit piezoelectricity are collagen, keratin and fibrin [65,133]. Piezoelectric polysaccharides are cellulose, chitin and amylose [133, 276, 277]. Collagen is a natural protein, found in living bone and due to its non-centrosymmetric structure, bone exhibits piezoelectricity [6,65]. Collagen has been proved as an excellent biocompatible material due to its reasonable cell binding ability and low antigenicity [92, 278]. Rocha et al. [279] observed earlier bone growth on hydrolysis-treated collagen implanted defect in rat's femur as compared to non-implanted defects. Similarly, hydrolysis treated collagen fibers also results in enhanced proliferation and differentiation of hFOB cells [280]. In addition, the collagen-based scaffold has been reported to support the functionality of SaOS-2 osteoblast-like cells [281]. Kakudo et al. [282] implanted 3D cultured hASC - honeycomb collagen composite scaffold on the subcutaneous mice tissue for 8 weeks. It has been revealed that the differentiation of hASC produces osteoblasts, which subsequently accelerates hard tissue formation. In addition, a bioactive glass - collagen composite scaffold has also been demonstrated to support the proliferation of MG-63 cells [283]. In the previous section, we have elaborated the addition of some natural polymers like collagen, cellulose induces the improved biological response of synthetic polymers, such as, PLLA, PHB, etc. [249,250,265]. However, high degradation rate and low stiffness of natural polymers put the concern on their mechanical strength [278, 284].

Chitosan is another piezoelectric natural polysaccharide polymer, as reviewed by Martino et al. [89]. It has been demonstrated that chitosan-based polymer scaffolds exhibit several favorable characteristics to be used as orthopedic implant such as, osteoconductivity,

**Table 4**

Biocompatibility of few selected piezoelectric polymers.

S-N.	Piezoelectric polymers/polymer-based composites	Fabrication/Processing route	In vitro/in vivo study	Key assessments	Ref.
1.	PVDF film	Polarized, 52 µm thick film	MC3T3-E1 pre-osteoblast cell, BCA protein adsorption	Increased cell viability, improved cell metabolism and protein adsorption on the polarized PVDF film from 24 h to 48 h	[231]
2.	PVDF film	Polarized and stretched, 20–30 µm thick film, the Solvent evaporation method	Fibronectin protein adsorption, MC3T3-E1 osteoblast cell response	Higher protein adsorption and a significant increase in cell density on the polarized polymer substrate as compared to the unpolarized substrate	[232], [233]
3.	PVDF microparticles	Microparticles produced by electrospray processing	MC3T3-E1 pre-osteoblast cell	Significant increase in cell viability as compared to control	[225]
4.	PVDF fibers	Electrospinning (@ 12–30 kV)	hMSC cell response	Higher ALP activity and early mineralization of extracellular matrix on PVDF fibers, electrospun at 25 kV as compared to that at 12 kV	[229]
5.	PVDF microparticles	Electrospray processing	hMSC cell response	PVDF film with spherical topography shows better cell viability as compared to film with flattened topography	[234]
6.	PVDF film	Solvent evaporation and melting, followed by stretching and polarization (@ 5 kV/cm)	Human adipose stem cells (hASC)	Significant increase in ALP activity on polarized PVDF surface as compared to unpolarized PVDF surfaces	[235], [236]
7.	PVDF film	28 µm thick piezoelectric PVDF film	Goat marrow cells	Significantly higher DNA content on the piezoelectric substrate under mechanical stimulation after 14 days of culture, higher ALP activity after 14 days	[237]
8.	PVDF film	Piezoelectric PVDF film, prepared by stretching and poling	Implantation in tibialis anterior of rat	Polarized substrate results in enhanced bone growth and significantly higher periosteal reaction	[41]
9.	PVDF film and fibers	Piezoelectric film and fibers (electrospun@ 25 kV) prepared by solvent casting, followed by corona poling	Implantation in the defected region of rat's femur	Piezoelectric scaffolds result in larger defect repair as compared to unpolarized scaffold after 4 weeks	[42]
10.	PVDF 3D nanofibers scaffold	Electrospinning, followed by oxygen plasma surface treatment	SaOS-2 cellular response	Oxygen plasma treatment enhances hydrophilicity and subsequent increase in cell viability of PVDF scaffold, over non-treated samples	[239]
11.	P(VDF-TrFE) 3D fibrous scaffold	Electrospinning method	hMSC cell response	Augmented cell proliferation, osteogenic differentiation, matrix mineralization, gene expression after 28 days	[240]
12.	P(VDF-TrFE) tube	Polarized tube with outside positively charged surface and inside negatively charged surface	Implantation in the mouse femur bone	Neobone growth at the inner negatively charged surface of the tube	[241]
13.	P(VDF-TrFE) – 10 vol% BaTiO <sub>3</sub> composite	Solid state mixing route	Implantation in rat calvarial for 8 weeks	Enhanced neobone formation in P(VDF-TrFE) - BT composite scaffold as compared to polytetrafluoroethylene (PTFE) polymer	[243]
14.	P(VDF-TrFE) – 5 vol% BaTiO <sub>3</sub> membrane	P(VDF-TrFE) - 5 vol % BT nanoparticles (coated with polydopamine) composite scaffold, prepared by solvent casting method, corona poling (@ 13 kV)	Rat bone marrow mesenchymal stem cells or rBMSCs response, implantation of nanocomposite on the calvarial defect of rat up to 12 weeks	Increased osteogenic differentiation after 7 days, Stimulated interfacial bone growth observed for polymer-ceramic membrane as compared to the monolithic polymer membrane	[28]
15.	P(VDF-TrFE) -BNNT (1 wt %) composite film	Cast-annealing method	SaOS-2 cells	Increased calcium deposition (osteogenic differentiation) after 7 days	[244]
16.	Poly (l-lactic acid) or PLLA thin film	Spin coating, followed by polarization (@ 50 V)	Fibronectin protein adsorption	Significantly higher protein adsorption on polarized films (90–450 nm protein aggregates) as compared to unpolarized film (45–136 nm protein aggregates)	[246]
17.	PLLA rods	PLLA drawn into rod shaped via extrusion to increase its piezoelectric response	Implantation in tibia bone of cats for 8 weeks	PLLA rods result in higher bone fracture repair as compared to polyethylene control	[247]
18.	PLLA film	Piezoelectric film	Implantation in periosteum of the tibial bone of rabbit up to 8 weeks	Neobone formation observed after 1 week, which matures by 8 weeks	[248]
19.	PLLA coated with HA/Collagen 3D porous scaffold	Phase-separation technique, followed by accelerated biomimetic coating	SaOS-2 cell response	Larger spreading of cells, significantly higher cell viability and ALP activity (more than 3 times) than PLLA and PLLA coated with HA	[249]
20.	HA/PLLA/collagen nanofiber composite	Electrospinning, weight ratio of PLLA:Collagen:HA is 40:40:20	hFOB cell proliferation, ALP activity	Significantly higher cell proliferation and ALP activity, 57% higher cell mineralization as compared to PLLA	[250]
21.	PLLA-DBP (Demineralized bone powder) nanofiber composite and PLLA	PLLA (prepared by electrospinning @ 18 kV) combined with DBP	hMSC, cultured in osteogenic medium	Significantly higher calcium deposition on the composite scaffolds ( $115 \pm 25 \mu\text{g}$ ) as	[251]

(continued on next page)

**Table 4 (continued)**

S-N.	Piezoelectric polymers/polymer-based composites	Fabrication/Processing route	In vitro/in vivo study	Key assessments	Ref.
22.	PLLA - DBP nanofiber composite and PLLA	PLLA (prepared by electrospinning @ 18 kV) combined with DBP Salt leaching method	Implantation in skull defects of rats	compared to PLLA scaffolds ( $33 \pm 6 \mu\text{g}$ ) after 14 days 90% of bone defect healed by composite scaffold, while only 70% by PLLA scaffold, after 12 weeks of implantation	[251]
23.	poly(3-hydroxybutyrate-co-3-hydroxyhexanoate) or PHBHH 3D scaffold	Additive manufacturing	Proliferation, differentiation of rabbit bone marrow cells	60% and 40% higher cell density than PLLA and PHB, respectively. 50% higher ALP activity than PLLA and PHB	[258]
24.	PHBHH or poly[(R)-3-hydroxybutyrate-(R)-3-Hydroxyhexanoate] 3D porous scaffold	Film and plate for implantation	MC3T3-E1 osteoblast cell response	Enhanced cell proliferation and osteogenic differentiation after 21 days	[87]
25.	PHB or Poly- $\beta$ -Hydroxybutyric Acid film and plate	Differentiation of hASC on the composite scaffold	Implantation in the osseous skull of rabbits	No inflammation and almost negligible decomposition of substitute material during implantation, complete fracture repair takes place after 25 months Neocartilage tissues after 24 days of implantation	[264]
26.	PHB-PHBHH 3D scaffold	Compounding - compression molding	hASC treated composite scaffold implanted in subcutaneous part of mice <i>in vitro</i> bioactivity	Composite with larger amount of HA results in rapid apatite growth	[266]
27.	PHB - (0–30 vol %) HA Composite scaffolds	Phase separation-solvent evaporation method	FBS protein adsorption, MC3T3-E1 osteoblast Cell response	Significantly higher protein and cell adhesion and almost double ALP activity than that of PHBHH scaffold	[262]
28.	PHB - HA 3D composite scaffold	Salt leaching method	Bone marrow cell response, ALP activity	Significantly higher cell proliferation and differentiation on PHB - HA scaffolds than PHB polymer	[259]
29.	PHBHH - (1 wt %) carbon nanotube Semiconductivenanocomposite film	Solution casting method	hMSC cell proliferation and osteogenic differentiation	A significant increase in hMSC proliferation and osteogenic differentiation (ALP activity, mineral content and osteoblast gene expression) on PHBHH - 1% CNT nanocomposite than PHBHH and PLLA films	[263]
31.	PHBHV [polyhydroxybutyrate-co-(3 hydroxyvalerate) having 2% valerate fraction] - HA (2–5 wt %) - silk fibroin (2–5 wt %) fibrous scaffold	Electrospinning (@ 10 kV)	Human osteoblast cell response	Higher Ca/P (1.75) ratio, and augmented cellular adhesion and proliferation on the composite scaffolds	[260]
32.	PHBHV [polyhydroxybutyrate-co-(3 hydroxyvalerate) having 8 mol. % valerate fraction]	Chondrocyte seeded on PHBHV matrix	Chondrocytes response; implantation in cartilage defect site of rabbit knee bone	Chondrocyte seeded PHBHV matrix exhibits higher cartilage defect repair than chondrocyte seeded collagen matrix	[265]
33.	Polyamide - HA (wt. ratio = 4:6) porous composite scaffold	Thermally induced phase inversion method	Rabbit BMSCs response	Increased cell proliferation on the scaffold up to 7 days and ALP activity increases almost 5 times on the 10th day of culture as compared to the first day	[270]
34.	Polyamide - HA (wt. ratio = 6 : 4) anisotropic (aligned fibers) porous scaffold	Thermally induced phase separation method	Cellular response using MG-63 cells	Anisotropic scaffolds with larger interconnected pores facilitate higher cell attachment and proliferation than isotropic composite scaffolds	[271]
35.	Polyamide - (5–10 wt %) HA composite scaffold	Selective laser sintering	MG-63 cell response	Enhanced cell growth and differentiation on composite scaffold than polyamide scaffold	[272]
36.	Polyamide - HA (wt. ratio = 4 : 6) porous composite scaffold	Prepared via thermally induced phase inversion method	Implantation in the jaw bone of the rabbit for 12 weeks	Mature bone observed at 8th week, bone at the defected region shows similar density as that of host bone after 12 weeks	[270]
37.	Polyamide 6 - HA (wt. ratio = 4 : 6) composite scaffold	Phase separation - particle leaching method	The response of rat BMSCs, followed by implantation of BMSCs treated scaffold in rat's calvarial defect	Early bone regeneration	[273]
38.	Polyamide - HA (wt. ratio = 6 : 4) anisotropic (aligned fibers) porous scaffold	Thermally induced phase separation method	Implantation in defected sites of bone in rabbit	Anisotropic scaffold with a large fraction of porosity (86.4%) facilitates almost double rate of tissue penetration as compared to isotropic scaffolds with lower porosity (80.2%)	[271]
39.	Polyamide 66 - HA - glass fiber (wt. ratio = 2 : 3: 5) composite	Injection molding method	Rat BMSCs response (proliferation, matrix mineralization, differentiation)	Accelerated proliferation and differentiation of BMSCs on the composite scaffold	[274]
40.	Polyamide (Nylon 6) - (1–2 wt %) PVA polymeric scaffold	Scaffold prepared by the deposition of PVA on the electrospinning processed nylon 6 nanofibers	MC3T3-E1 osteoblast cell attachment	PVA deposited scaffolds result in increase in the adherence of MC3T3-E1 pre-osteoblast cells as compared to nylon 6 scaffold	[88]
41.	polyamide 66 - (10–20 wt %) chitosan Nanofiber scaffold	Co-Electrospinning technique	MC3T3-E1 osteoblast cell response	Viability of MC3T3-E1 osteoblast cells increases with increasing the amount of chitosan	[275]
42.	Collagen fibers	Hydrolysis treatment on the collagen fibrils	Implantation in rat's tibia	Collagen implanted defects were filled with cancellous bone; however empty defect	[279]

(continued on next page)

**Table 4 (continued)**

S-N.	Piezoelectric polymers/polymer-based composites	Fabrication/Processing route	In vitro/in vivo study	Key assessments	Ref.
43.	Collagen fibers	Hydrolysis treatment on the collagen fibrils	hFOB cell response	was repaired by cortical bone, after one month of implantation Enhanced osteogenic proliferation and differentiation on hydrolysis treated collagen on scaffolds	[280]
44.	Collagen fibrils-based 3D matrix scaffold	Honeycomb shaped scaffold, prepared by crosslinking method	hASC response, implantation of hASC embedded collagen scaffold in the subcutaneous tissue of mice for 8 weeks	Almost 3 times increase in ALP activity from 7 to 14 days, the differentiation of hASC into osteoblasts observed on hASC embedded collagen matrix	[282]
45.	Type-1 collagen - (20–40 wt %) 58SiO <sub>2</sub> -38CaO-4P <sub>2</sub> O <sub>5</sub> ) electrospun bioactive glass porous nanocomposite scaffold	Thin membrane and macroporous scaffold, prepared by mold pressing and solution casting, respectively	MG-63 cell response	Composite scaffolds show higher cell growth and significantly higher ALP activity (differentiation) than that of collagen membrane	[283]
46.	Chitosan polymer	Chitosan polymer with varying degree of acetylation (4–49%)	MG-63 cell response	Chitosan with less than 13% of the degree of acetylation results in significantly higher cell proliferation and differentiation	[90]
47.	Cellulose porous scaffold	Scaffold prepared by incorporation of paraffin wax with bacterial cellulose via fermentation process	MC3T3-E1 osteoblast response	Higher cell proliferation and mineralization on the wax-cellulose composite scaffold as compared to bacteria cellulose scaffold	[91]

porosity, easy molding ability, antibacterial response and minimum foreign body reaction [89]. Cellulose is another piezoelectric polysaccharide natural polymer, which can be a suitable candidate for bone tissue applications due to its superior biocompatibility and good mechanical strength. Zaborowska et al. [91] observed that cellulose-based microporous scaffold results in significantly higher proliferation of MC3T3-E1 osteoblast cells as compared to the nanoporous scaffold.

## 5. Opportunity and challenges

As discussed above, the piezoelectricity induced biocompatibility has been explored for a limited number of piezoresponsive biomaterials (for example, HA-NKN, HA-BaTiO<sub>3</sub>, piezopolymers- BaTiO<sub>3</sub>, MgSiO<sub>3</sub>-polymers etc.). Surface charge facilitates apatite formation, cell growth and proliferation, osseointegration etc. The optimization of poling conditions including temperature, electric field, time and corresponding surface charge to modulate different cell fate processes (cell adhesion, differentiation, proliferation etc.) is quite challenging as far as the mapping of surface charge is concerned. Another approach could be to examine the efficiency of highly intense laser sources in order to establish a dynamic poling of electroactive composites, and subsequently, study osteogenesis on such laser-treated surfaces.

Concerning the piezoelectric material-based therapy for bone tissue engineering, synergistic interaction among the electric field stimulation and piezoelectric properties should be explored to assess the potential to guide mesenchymal cells towards osteogenesis, contributing to bone growth. The questions, remain to be addressed, are related to the specific mechanisms of stem cell activation by external electrical stimuli. In this approach, one of the major challenges is to tailor the critical amount of piezoelectric phase to enhance the biocompatibility. It is also known that the piezoelectric strain coefficients are dependent on the physical structure, e.g. fiber, film and bulk phase of the same biocompatible material can have different piezoelectricity. Towards this end, it would be important to establish the tuning between the shape of the piezoelectric material and biocompatibility. The outcome of such research programs will have significant relevance for the emerging field of Regenerative Engineering.

The structure-property correlation in many piezoelectric bioceramics is not well established. To this end, synchrotron facility, i.e. extended X-ray absorption spectroscopy (EXAFS) can be explored to record high resolution data for compositionally tailored multicomponent bioceramics. This together with computational techniques, like molecular dynamics simulation, Density Functional Theory (DFT) can be used to precisely determine the atomic positions of different elements in

biocompatible piezoceramics (often having complex crystal structure). Such analysis would pave the way for the design of new piezoelectric composites.

While evaluating cytocompatibility, it would be important to co-culture endothelial cells with bone tissue-specific cells, in efforts to facilitate better maturation of engineered tissues. Another recommended approach would be to adopt the biomicrofluidic technology, wherein *in vitro* experiments can be carried out in designed lab-on-chip devices under physiologically relevant shear, together with the application of tailored electrical stimuli.

The bench-to-bed translation in the context of tissue engineering and regenerative medicine is another aspect that needs further investigation. Although, a multitude of *in vitro* studies are being reported in literature, translational research would require more pre-clinical studies, with microelectronic miniaturised modules to deliver electrical stimulation, followed by thoughtful clinical trials. This will impact the growth of the field of Bioelectronic Medicine.

In the context of biocompatibility testing, it is equally important to assess the genotoxicity of the piezoelectric biomaterials in a size and dose dependent manner, using comet assay, single cell gel electrophoresis or micronucleus (flow cytometry) techniques. The quantitative analyses together with the mechanism of DNA fragmentation have large significance for epigenetic changes. This obviates the necessity of evaluating genotoxic, epigenetic, and carcinogenic effects, to improve the clinical acceptability of the class of piezoelectric biomaterials.

## 6. Summary

This review article presents the fundamental aspects of bioelectrical phenomenon in natural bone. The piezoelectricity has been demonstrated as an intrinsic functional property to regulate bone metabolism. In a continuous surge towards bone mimicking materials, the development of piezoelectric bioceramics and biopolymers has been discussed herein for bone tissue engineering applications. Towards this end, a number of processing related challenges, such as, densification, volatilization of alkali elements for a range of compositionally tuned piezoelectric bioceramics, in particular reference to sodium potassium niobate, have been discussed. Importantly, the piezoelectricity/electrical stimulation induced augmented bioactivity, cellular response, tissue regeneration, etc. have been highlighted with a specific emphasis on the biocompatibility of polarized piezoelectric bioceramics and biopolymers.

It needs to be emphasized as how piezoelectric and electrically conducting materials together with external stimulation form the basis

of new, interesting and efficient strategies for bone tissue engineering and regenerative medicine applications. Owing to the number of advantages associated with piezoelectric biomaterials (piezoelectricity, pyroelectricity as well ferroelectricity), and biological (poling induced mineralization and cellular) response, it is envisaged that piezoelectric biomaterials could serve as orthopedic implant materials in near future. The fundamental principles that drive the synergistic interactions among substrate properties and stimulation parameters to govern cell-material interactions are still unknown. This is an area, which can be benefitted by multiscale computational analyses.

Also, more pre-clinical studies in larger animal models are to be conducted on piezobiomaterials, which can be followed by clinical trials in human subjects. We strongly believe that the potential of the implantable piezoelectric materials for bone repair and regeneration will open up a new gateway for bone tissue engineering applications.

### Declaration of competing interest

The authors declare that they have no known competing financial interests or personal relationships that could have appeared to influence the work reported in this paper.

### Acknowledgments

The financial support from SERB, DST, Govt. of India is gratefully acknowledged. BB acknowledges the support from the Department of Biotechnology under the program of 'Translational Center of Excellence on Biomaterials for Orthopedic and Dental applications' and "Bioengineering and Biodesign Initiative" Dept. of Biotechnology, Govt. of India. We thank Nandita Keshavan for help in editing a few figures.

### References

- [1] E. Fukada, I. Yasuda, On the piezoelectric effect of bone, *J. Phys. Soc. Japan* 12 (1957) 1158–1162.
- [2] M.A.E. Messier, G.W. Hastings, S. Rakowski, Ferro-electricity of dry cortical bone, *J. Biomed. Eng.* 1 (1979) 63–65.
- [3] S.B. Lang, Pyroelectricity: occurrence in biological materials and possible physiological implications, *Ferroelectrics* 34 (1981) 3–9.
- [4] C.S. McDowell, Implanted Bone Stimulator and Prosthesis System and Method of Enhancing Bone Growth, U.S Patent, 2000, p. 6143035A.
- [5] F.R. Baxter, C.R. Bowen, I.G. Turner, A.C.E. Dent, Electrically active bioceramics: a review of interfacial responses, *Ann. Biomed. Eng.* 38 (2010) 2079–2092.
- [6] G.W. Hastings, F.A. Mahmud, Electrical effects in bone, *J. Biomed. Eng.* 10 (1988) 515–521.
- [7] C. Halperin, S. Mutchnik, A. Agronin, M. Molotskii, P. Urenski, M. Salai, G. Roseman, Piezoelectric effect in human bones studied in nanometer scale, *Nano Lett.* 4 (2004) 1253–1256.
- [8] S.B. Lang, Pyroelectric effect in bone and tendon, *Nature* 212 (1966) 704–705.
- [9] C.D. McCaig, M. Zhao, Physiological electrical fields modify cell behavior, *Bioessays* 19 (1997) 819–826.
- [10] I. Yasuda, Electrical callus and callus formation by electret, *Clin. Orthop. Relat. Res.* 124 (1977) 53–56.
- [11] C.A.L. Bassett, R.O. Becker, Generation of electric potentials by bone in response to mechanical stress, *Science* 137 (1962) 1063–1064.
- [12] B.M. Isaacson, R.D. Bloebaum, Bone bioelectricity: what have we learned in the past 160 years? *J. Biomed. Mater. Res.* 95A (2010) 1270–1279.
- [13] A.G. Robling, C.H. Turner, Mechanical signaling for bone modeling and remodeling, *Crit. Rev. Eukaryot. Gene Expr.* 19 (2009) 319–338.
- [14] Z.B. Friedenberg, C.T. Brighton, Bioelectric potentials in bone, *J. Bone Joint Surg. Am.* 48 (1966) 915–923.
- [15] A.C. Ahn, A.J. Grodzinsky, Relevance of collagen piezoelectricity to "Wolff's Law": a critical review, *Med. Eng. Phys.* 31 (2009) 733–741.
- [16] A.K. Dubey, S.D. Gupta, B. Basu, Optimization of electrical stimulation parameters for enhanced cell proliferation on biomaterial surfaces, *J. Biomed. Mater. Res.* 98B (2011) 18–29.
- [17] A.K. Dubey, B. Basu, Pulsed electrical stimulation and surface charge induced cell growth on multistage spark plasma sintered hydroxyapatite barium titanate piezobiocomposite, *J. Am. Ceram. Soc.* 97 (2014) 481–489.
- [18] G. Thriyikraman, G. Madras, B. Basu, Intermittent electrical stimuli for guidance of human mesenchymal stem cell lineage commitment towards neural-like cells on electroconductive substrates, *Biomaterials* 35 (2014) 6219–6235.
- [19] G. Thriyikraman, P. Lee, R. Hess, V. Haenchen, B. Basu, D. Scharnweber, Interplay of substrate conductivity, cellular microenvironment and pulsatile electrical stimulation towards osteogenesis of human mesenchymal stem cells *in vitro*, *ACS Appl. Mat. Interf.* 7 (2015) 23015–23028.
- [20] K. Ravikumar, G.P. Kar, S. Bose, B. Basu, Synergistic effect of polymorphism, substrate conductivity and electric field stimulation towards muscle cell growth *in vitro*, *RSC Adv.* 6 (2016) 10837–10845.
- [21] K. Ravikumar, S.K. Boda, B. Basu, Synergy of substrate conductivity and intermittent electrical stimulation towards osteogenic differentiation of human mesenchymal stem cells, *Bioelectrochemistry* 116 (2017) 52–64.
- [22] S. Naskar, V. Kumaran, B. Basu, Reprogramming the stem cell behaviour by shear stress and electric field modulation: lab-on-a-chip based applications in regenerative medicine, *Reg. Eng. Transl. Med.* (2018) 1–29.
- [23] G. Thriyikraman, S.K. Boda, B. Basu, Unravelling the mechanistic effects of electric field stimulation towards directing stem cell fate and function: a tissue engineering perspective, *Biomaterials* 150 (2018) 60–86.
- [24] K. Ravikumar, V. Kumaran, B. Basu, Biophysical implications of Maxwell stress in electric field stimulated cellular microenvironment on biomaterial substrates, *Biomaterials* 209 (2019) 54–66.
- [25] M.E. Mycielska, M.B.A. Djamgoz, Cellular mechanisms of direct-current electric field effects: galvanotaxis and metastatic disease, *J. Cell Sci.* 117 (2009) 1631–1639.
- [26] A.K. Dubey, A. Mukhopadhyay, B. Basu, *Interdisciplinary Engineering Sciences: Concepts and Applications*, CRC Press (Taylor and Francis Group, UK, 2020), p. 358. ISBN: 978-0-3673-3393-5.
- [27] A.H. Rajabi, M. Jaffe, T.L. Arinze, Piezoelectric materials for tissue regeneration: a review, *Acta Biomater.* 24 (2015) 12–23.
- [28] X. Zhang, C. Zhang, Y. Lin, P. Hu, Y. Shen, K. Wang, S. Meng, Y. Chai, X. Dai, X. Liu, Y. Liu, X. Mo, C. Cao, S. Li, X. Deng, L. Chen, Nanocomposite membranes enhance bone regeneration through restoring physiological electric microenvironment, *ACS Nano* 10 (2016) 7279–7286.
- [29] C. Ribeiro, V. Sencadas, D.M. Correia, S. Lanceros-Mendez, Piezoelectric polymers as biomaterials for tissue engineering applications, *Colloids Surf. B Biointerfaces* 136 (2015) 46–55.
- [30] J. Jacob, N. More, K. Kalia, G. Kapusetti, Piezoelectric smart biomaterials for bone and cartilage tissue engineering, *Inflamm. Regen.* 38 (2018).
- [31] B. Tandon, J. Blaker, S. Cartmell, Piezoelectric materials as stimulatory biomedical materials and scaffolds for bone repair, *Acta Biomater.* 73 (2018) 1–20.
- [32] B. Basu, *Biomaterials Science and Tissue Engineering: Principles and Methods*, first ed., Cambridge University Press, 2017, p. 716. ISBN: 9781108415156.
- [33] T. Eriksson, K. Nelsson, A.-K. Johansson, K. Ljungstrom, K. Lashgari, A. Pohl, G. Westin, Synthesis of Sodium potassium niobate by sol gel, Patent No. US 8 (2012), 246,929 B2.
- [34] S.R. Platt, S. Farritor, K. Garvin, H. Haider, The use of piezoelectric ceramics for electric power generation within orthopedic implants, *IEEE Trans. Mechatron.* 10 (2005) 455–461.
- [35] M.T. Chorsi, E.J. Curry, H.T. Chorsi, R. Das, J. Baroody, P.K. Purohit, H. Ilies, T. D. Nguyen, Piezoelectric biomaterials for sensors and actuators, *Adv. Mater.* 31 (2019) 1802084.
- [36] A. Sultana, S.K. Ghosh, V. Sencadas, T. Zheng, M.H. Higgins, T.R. Middya, D. Mandal, Human skin interactive self-powered wearable piezoelectric bio-e-skin by electrospun poly-L-lactic acid nanofibers for non-invasive physiological signal monitoring, *J. Mater. Chem. B* 5 (2017) 7352–7359.
- [37] J.H. McElhaney, The charge distribution on the human femur due to load, *J. Bone Joint Surg. Am.* 49 (1967) 1561–1571.
- [38] J.B. Park, A.F. von Recum, G.H. Kenner, B.J. Kelly, W.W. Coffeen, M.F. Grether, Piezoelectric ceramic implants: a feasibility study, *J. Biomed. Mater. Res.* 14 (1980) 269–277.
- [39] K.S. Hwang, J.E. Song, H.S. Yang, Y.J. Park, J.L. Ong, H.R. Rawls, Effect of poling conditions on growth of calcium phosphate crystal in ferroelectric BaTiO<sub>3</sub> ceramics, *J. Mater. Sci. Mater. Med.* 13 (2002) 133–138.
- [40] N. More, G. Kapusetti, Piezoelectric material - a promising approach for bone and cartilage regeneration, *Med. Hypotheses* 108 (2017) 10–16.
- [41] A. Marino, J. Rosson, E. Gonzalez, L. Jones, S. Rogers, E. Fukada, Quasi static charge interactions in bone, *J. Electrost.* 21 (1988) 347–360.
- [42] C. Ribeiro, D.M. Correia, I. Rodrigues, L. Guardão, S. Guimarães, R. Soares, S. Lanceros-Méndez, *In-vivo* demonstration of the suitability of piezoelectric stimuli for bone reparation, *Mater. Lett.* 209 (2017) 118–121.
- [43] K. Kapat, Q.T.H. Shubhra, M. Zhou, S. Leeuwenburgh, Piezoelectric nanobiomaterials for biomedicine and tissue regeneration, *Adv. Funct. Mater.* (2020) 1909045.
- [44] G. Murillo, A. Blanquer, C. Vargas-Estevez, L. Barrios, E. Ibáñez, C. Nogués, J. Esteve, Electromechanical nanogenerator-cell interaction modulates cell activity, *Adv. Mater.* 29 (2017) 1605048.
- [45] Y. Liu, X. Zhang, C. Cao, Y. Zhang, J. Wei, Y. Li, W. Liang, Z. Hu, J. Zhang, Y. Wei, X. Deng, Built-In electric fields dramatically induce enhancement of osseointegration, *Adv. Funct. Mater.* 27 (2017) 1703771.
- [46] T. Zigman, S. Davila, I. Dobric, T. Antoljak, G. Augustin, D. Rajacic, T. Kovac, T. Ehrenfreund, Intraoperative measurement of bone electrical potential: a piece in the puzzle of understanding fracture healing, *Injury* 44 (2013) S16–S19.
- [47] B. Dutta, E. Kar, N. Bose, S. Mukherjee, NiO@SiO<sub>2</sub>/PVDF: a flexible polymer nanocomposite for high performance human body motion based energy harvester and tactile e-skin mechanosensor, *ACS Sustain. Chem. Eng.* 6 (2018) 10505–10516.
- [48] H. He, Y. Fu, W. Zang, Q. Wang, L. Xing, Y. Zhang, X. Xue, A flexible self-powered T-ZnO/PVDF/fabric electronic-skin with multi-functions of tactile-perception, atmosphere detection and self-clean, *Nanomat.* Energy 31 (2017) 37–48.
- [49] T. Huang, S. Yang, P. He, J. Sun, S. Zhang, D. Li, Y. Meng, J. Zhou, H. Tang, J. Liang, G. Ding, X. Xie, Phase-separation-induced PVDF/graphene coating on

- fabrics toward flexible piezoelectric sensors, *ACS Appl. Mater. Interfaces* 10 (2018) 30732–30740.
- [50] A. Wang, Z. Liu, M. Hu, C. Wang, X. Zhang, B. Shi, Y. Fan, Y. Cui, Z. Li, K. Ren, Piezoelectric nanofibrous scaffolds as *in vivo* energy harvesters for modifying fibroblast alignment and proliferation in wound healing, *Nanomater. Energy* 43 (2018) 63–71.
- [51] D.B. Jensen, Z. Li, I. Pavel, E. Dervishi, A.S. Biris, A.R. Biris, D. Lupu, P.J. Jensen, Bone tissue: a relationship between micro and nano structural composition and its corresponding electrostatic properties with applications in tissue engineering, *IEEE* (2007) 55–59.
- [52] C.A.L. Bassett, S.N. Mitchell, S.R. Gaston, Treatment of ununited tibial diaphyseal fractures with pulsing electromagnetic fields, *J. Bone Joint Surg.* 63-A (1981) 511–523.
- [53] B. Amin, M.A. Elahi, A. Shahzad, E. Porter, M. O'Halloran, A review of the dielectric properties of the bone for low frequency medical technologies, *Biomed. Phys. Eng. Express* 5 (2019), 022001.
- [54] R. Cappanna, D. Donati, C. Masetti, M. Manfrini, A. Panizzo, R. Cadossi, M. Campanacci, Effect of electromagnetic fields on patients undergoing massive bone grafts following bone tumor resection, *Clin. Orthop. Relat. Res.* 306 (1994) 213–221.
- [55] J. Behari, H. Kumar, R. Aruna, Effect of ultraviolet light on the dielectric behavior of bone at microwave frequencies, *Ann. Biomed. Eng.* 10 (1982) 139–144.
- [56] A. Ivancich, J.R. Grigera, C. Muravchik, Electric behaviour of natural and demineralized bones. Dielectric properties up to 1 GHz, *J. Biol. Phys.* 18 (1992) 281–295.
- [57] G.B. Reinish, A.S. Nowick, Effect of moisture on the electrical properties of bone, *J. Electrochem. Soc.: Electrochem. Sci. techn.* 123 (1976) 1451–1455.
- [58] P.M. Meaney, T. Zhou, D. Goodwin, A. Golnabi, E.A. Attardo, K.D. Paulsen, Bone dielectric property variation as a function of mineralization at microwave frequencies, *Int. J. Biomed. Imag.* 2012 (2012) 649612. Article ID.
- [59] M.H. Shamos, L.S. Lavine, Physical bases for bioelectric effects in mineralized tissues, *Clin. Orthopaed.* 35 (1964) 177–188.
- [60] S. Singh, S. Saha, Electrical properties of bone: a review, *Clin. Orthop. Relat. Res.* 186 (1984) 249–271.
- [61] X. Gao, I. Sevostianov, Connection between elastic and electrical properties of cortical bone, *J. Biomech.* 49 (2016) 765–772.
- [62] K.C. Kao, Dielectric Phenomenon in Solids, Book Elsevier Acad. Press, 2004, p. 215. ISBN: 0-12-396561-6.
- [63] R.E. Newnham, Properties of Materials, Book Oxford university press, 2005, p. 176. ISBN 0-19-852075-1 (hbk) ISBN 0-19-852076-x (pbk).
- [64] M. Minary-Jolandan, M.F. Yu, Shear piezoelectricity in bone at the nanoscale, *Appl. Phys. Lett.* 97 (2010) 153127.
- [65] E. Fukada, I. Yasuda, Piezoelectric effects in collagen, *Jpn. J. Appl. Phys.* 3 (1964) 117–121.
- [66] C. Turner, T. Wang, D. Burr, Shear strength and fatigue properties of human cortical bone determined from pure shear tests, *Calc. tiss. int.* 69 (2002) 373–378.
- [67] G.N. Ramachandran, G. Kartha, Structure of collagen, *Nature* 174 (1954) 269–270.
- [68] G.W. Hastings, ELMessiery Ma, S. Rakowsk, Mechano-electric properties of bone, *Biomaterials* 2 (1981) 225–233.
- [69] K. Nelsson, J. Lidman, K. Ljungstrom, C. Kjellman, Biocompatible Material for Implants, Patent No. US 6526984 B1, 2003.
- [70] W. Chen, Z. Yu, J. Pang, P. Yu, G. Tan, C. Ning, Fabrication of biocompatible potassium sodium niobate piezoelectric ceramic as an electroactive implant, *Materials* 10 (2017) 18–21.
- [71] A. Jalalian, A.M. Grishin, Biocompatible ferroelectric (Na, K)NbO<sub>3</sub>, *Appl. Phys. Lett.* 100 (2012), 012904.
- [72] J.B. Park, B.J. Kelly, G.H. Kenner, A.F. von Recum, M.F. Grether, W.W. Coffeen, Piezoelectric ceramic implants: *In vivo* results, *J. Biomed. Mater. Res.* 15 (1981) 103–110.
- [73] G. Ciofani, L. Ricotti, V. Mattoli, Preparation, characterization and *in vitro* testing of poly (lactic-co-glycolic) acid/barium titanate nanoparticle composites for enhanced cellular proliferation, *Biomed. Microdevices* 13 (2011) 255–266.
- [74] A.K. Dubey, B. Basu, K. Balani, R. Guo, A.S. Bhalla, Multifunctionality of perovskites BaTiO<sub>3</sub> and CaTiO<sub>3</sub> in a composite with hydroxyapatite as orthopaedic implant materials, *Integrated Ferroelectrics Int. J.* 131 (2011) 119–126.
- [75] Q. Wang, X. Chen, J. Zhu, B.W. Darvell, Z. Chen, Porous Li-Na-K niobate bone-substitute ceramics: microstructure and piezoelectric properties, *Mater. Lett.* 62 (2008) 3506–3508.
- [76] Q. Wang, J. Yang, W. Zhang, R. Khoie, Y. Li, J. Zhu, Z. Chen, Manufacture and cytotoxicity of a lead-free piezoelectric ceramic as a bone substitute consolidation of porous lithium sodium potassium niobate by cold isostatic pressing, *Int. J. Oral Sci.* 1 (2009) 99–104.
- [77] A.K. Dubey, H. Yamada, K. Kakimoto, Space charge polarization induced augmented *in vitro* bioactivity of piezoelectric (Na,K) NbO<sub>3</sub>, *J. Appl. Phys.* 114 (2013) 124701.
- [78] N.C. Carville, L. Collins, M. Manzo, K. Gallo, B.I. Lukasz, K.K. McKayed, J. C. Simpson, B.J. Rodriguez, Biocompatibility of ferroelectric lithium niobate and the influence of polarization charge on osteoblast proliferation and function, *J. Biomed. Mater. Res.* 103A (2015) 2540–2548.
- [79] P. Vanek, Z. Kolska, T. Luxbacher, J.A.L. García, M. Lehocky, M. Vandrovcová, L. Bacakovaand, J. Petzelt, Electrical activity of ferroelectric biomaterials and its effects on the adhesion, growth and enzymatic activity of human osteoblast-like cells, *J. Phys. D Appl. Phys.* 49 (2016) 175403.
- [80] Z. Wu, T. Tang, H. Guo, S. Tang, Y. Niu, J. Zhang, W. Zhang, R. Ma, J. Su, C. Liu, J. Wei, In *Vitro* Degradability, Biocompatibility and Cell Responses to Mesoporous Magnesium Silicate for the Induction of Bone Regeneration, vol. 120, Elsevier: Coll. Sur. B: Biointer., 2014, pp. 38–46.
- [81] Z. Wu, K. Zheng, J. Zhang, T. Tang, H. Guo, A.R. Boccaccini, J. Wei, Effects of magnesium silicate on mechanical property, biocompatibility, bioactivity, degradability, osteogenesis of poly(butylene succinate) - based composite scaffolds for bone repair, *J. Mater. Chem. B (RSC)* 4 (2016) 7974–7988.
- [82] Y.G. Kang, J. Wei, J.W. Shin, Y.R. Wu, J. Su, Y.S. Park, J.W. Shin, Enhanced biocompatibility and osteogenic potential of mesoporous magnesium silicate/polycaprolactone/wheat protein composite scaffolds, *Int. J. Nanomed.* 13 (2018) 1107–1117.
- [83] J.G. Fisher, U.T. Thuan, M.U. Farooq, G. Chandrasekaran, Y.D. Jung, E.C. Hwang, J.-J. Lee, V.-K. Lakshmanan, Prostate cancer cell-specific cytotoxicity of sub-micron potassium niobate powder, *J. Nanosci. Nanotechnol.* 18 (2018) 3141–3147.
- [84] X. Li, W. Xiupeng, X. Jiang, M. Yamaguchi, A. Ito, Y. Bando, D. Golberg, Boron nitride nanotube-enhanced osteogenic differentiation of mesenchymal stem cells, *J. Biomed. Mater. Res. B Appl. Biomater.* 104 (2015) 323–329.
- [85] C. Khatua, S. Bodhak, B. Kundu, V.K. Balla, *In vitro* bioactivity and bone mineralization of bismuth ferrite reinforced bioactive glass composites, *Materialia* 4 (2018) 361–366.
- [86] G. Narayanan, E. Kuyinu, Poly (lactic acid)-based biomaterials for orthopaedic regenerative engineering, *Adv. Drug Deliv. Rev.* 107 (2016) 247–276.
- [87] C. Mota, S.Y. Wang, D. Puppi, M. Gazzarrini, C. Migone, F. Chiellini, G.Q. Chen, E. Chiellini, Additive manufacturing of poly[(R)-3-hydroxybutyrate-co-(R)-3-hydroxyhexanoate] scaffolds for engineered bone development, *J. Tiss. Eng. Regen. Med.* 11 (2017) 175–186.
- [88] A.H. Abdalla, S.H. Abdel, A.K. Khalil, Fabrication of durable high performance hybrid nanofiber scaffolds for bone tissue regeneration using a novel, simple *in situ* deposition approach of polyvinylalcohol on electrospun nylon 6 nanofibers, *Mater. Lett.* 147 (2015) 25–28.
- [89] D. martino, M. Sittinger, M.V. Risbud, Chitosan: a versatile biopolymer for orthopaedic tissue-engineering, *Biomater* 26 (2005) 5983–5990.
- [90] I. Amaral, A.L. Cordeiro, P. Sampaio, M. Barbosa, Attachment, spreading and short-term proliferation of human osteoblastic cells cultured on chitosan films with different degrees of acetylation, *J. Biomater. Sci. Polym. Ed.* 18 (2007) 469–485.
- [91] M. Zaborowska, A. Bodin, H. Backdahl, J. Popp, A. Goldstein, P. Gatenholm, Microporous bacterial cellulose as a potential scaffold for bone regeneration, *Acta Biomater.* 6 (2010) 2540–2547.
- [92] C.H. Lee, A. Singla, Y. Lee, Biomedical applications of collagen, *Int. J. Pharm.* 221 (2001) 1–22.
- [93] R.E. Jaeger, L. Egerton, Hot pressing of potassium sodium Niobates, *J. Am. Ceram. Soc.* 45 (1962) 209–213.
- [94] K. Kakimoto, Y. Hayakawa, I. Kagomiya, Low-temperature sintering of dense (Na, K)NbO<sub>3</sub> piezoelectric ceramics using the citrate precursor technique, *J. Am. Ceram. Soc.* 93 (2010) 2423–2426.
- [95] D. Berlincourt, H. Jaffe, Elastic and piezoelectric coefficients of single-crystal barium titanate, *Phys. Rev.* 111 (1958) 143–148.
- [96] H.B. Sharma, A. Mansingh, Sol-gel processed barium titanate ceramics and thin films, *Journal of material science* 33 (1998) 4455–4459.
- [97] T. Kimura, Q. Dong, S. Yin, T. Hashimoto, A. Sasaki, T. Sato, Synthesis and piezoelectric properties of Li-doped BaTiO<sub>3</sub> by a solvothermal approach, *J. Eur. Ceram. Soc.* 33 (2013) 1009–1015.
- [98] D. Xue, Y. Zhou, H. Bao, C. Zhou, J. Gao, Elastic, piezoelectric, and dielectric properties of Ba(Zr<sub>0.2</sub>Ti<sub>0.8</sub>O<sub>3</sub>)<sub>50</sub>(Ba<sub>0.7</sub>Ca<sub>0.3</sub>)TiO<sub>3</sub> Pb-free ceramic at the morphotropic phase boundary, *J. Appl. Phys.* 109 (2011), 054110.
- [99] S.B. Lang, Pyroelectricity: from ancient curiosity to modern imaging tool, *Phys. Today* 58 (2005) 31–36.
- [100] C. Chen, J. Ji, X. Jiao, H. Ding, Fabrication and properties of lithium sodium potassium niobate lead-free piezoelectric ceramics, *J. Adv. Microsc. Res.* 12 (2017) 85–88.
- [101] J. Parravicini, J. Saifiou, V. Degiorgio, P. Minzioni, M. Chauvet, All-optical technique to measure the pyroelectric coefficient in electro-optic crystals, *J. Appl. Phys.* 109 (2011), 033106.
- [102] S.C. Bhatt, B.S. Semwal, Dielectric and ultrasonic properties of LiNbO<sub>3</sub> ceramics, *Solid State Ionics* 23 (1987) 77–80.
- [103] E. Nakamachi, Y. Okuda, S. Kumazawa, Y. Uetsuji, K. Tsuchiya, H. Nakayasu, Development of fabrication technique of bio-compatible piezoelectric material MgSiO<sub>3</sub> by using helicon wave plasma sputter, *Trans. Jpn. Soc. Mech. Eng. Ser. A* 72 (2006) 353–358.
- [104] H. Nagata, K. Matsumoto, T. Hirosue, Y. Hiruma, T. Takenaka, Fabrication and electrical properties of potassium niobate ferroelectric ceramics, *Jpn. J. Appl. Phys.* 46 10 B (2007) 7084–7088.
- [105] H. Birol, D. Damjanovic, N. Setter, Preparation and characterization of KNbO<sub>3</sub> ceramics, *J. Am. Ceram. Soc.* 88 (2005) 1754–1759.
- [106] J.A. Bur, Measurements of dynamic piezoelectric properties of bone as a function of temperature and humidity, *J. Biomech.* 9 (1976) 495–507.
- [107] M. Chaari, Structural and dielectric properties of sintering zinc oxide bulk ceramic, *Mater. Sci. Appl.* 2 (2011) 764–769.
- [108] D.F. Crisler, J.J. Cupal, A.R. Moore, Dielectric, piezoelectric, and electromechanical coupling constants of zinc oxide crystals, *Proc. IEEE* 56 (1968) 225–226.





- [228] K.C. Satyanarayana, K. Bolton, Molecular dynamics simulations of  $\alpha$ - to  $\beta$ -poly(vinylidene fluoride) phase change by stretching and poling, *Polymer* 53 (2012) 2927–2934.
- [229] S.M. Damaraju, S. Wu, M. Jaffe, T.L. Arinze, Structural changes in PVDF fibers due to electrospinning and its effect on biological function, *Biomed. Mater.* 8 (2013), 045007.
- [230] D. Mandal, S. Yoon, K.J. Kim, Origin of piezoelectricity in an electrospun poly(vinylidene fluoride-trifluoroethylene) nanofiber web-based nanogenerator and nano-pressure sensor, *Macromol. Rapid Commun.* 32 (2011) 831–837.
- [231] C. Frias, J. Reis, F. Capela e Silva, J. Potes, J. Simões, A.T. Marques, Polymeric piezoelectric actuator substrate for osteoblast mechanical stimulation, *J. Biomech.* 43 (2010) 1061–1066.
- [232] C. Ribeiro, S. Moreira, V. Correia, V. Sencadas, J.G. Rocha, F.M. Gama, J.L. G. Ribelles, S.L. Mendez, Enhanced proliferation of preosteoblastic cells by dynamic piezoelectric stimulation, *RSC Adv.* 2 (2012) 11504–11509.
- [233] C. Ribeiro, J.A. Panadero, V. Sencadas, S.L. Mendez, M.N. Tamano, D. Moralat, M. S. Sanchez, J.L.G. Ribelles, Fibronectin adsorption and cell response on electroactive poly(vinylidene fluoride) films, *Biomed. Mater.* 7 (2012), 035004.
- [234] R.S. Almeida, M.T. Machiavello, E. Carvalho, L. Cordón, S. Doria, L. Senent, D. Correia, C. Ribeiro, S.L. Mendez, R. Sabater I. Serra, J.G. Ribelles, A. Sempere, Human mesenchymal stem cells growth and osteogenic differentiation on piezoelectric poly(vinylidene fluoride) microsphere substrates, *Int. J. Mol. Sci.* 18 (2017) 2391.
- [235] J. Parssinen, H. Hammaren, R. Rahikainen, V. Sencadas, C. Ribeiro, S. Vanhatupa, S. Miettinen, S. Lanceros-Mendez, V.P. Hytonen, Enhancement of adhesion and promotion of osteogenic differentiation of human adipose stem cells by poled electroactive poly(vinylidene fluoride), *J. Biomed. Mater. Res.* 103 (2015) 919–928.
- [236] C. Ribeiro, J. Parssinen, V. Sencadas, V. Correia, S. Miettinen, V.P. Hytonen, S. Lanceros-Méndez, Dynamic piezoelectric stimulation enhances osteogenic differentiation of human adipose stem cells, *J. Biomed. Mater. Res.* 103 (2015) 2172–2175.
- [237] M.T. Rodrigues, M.E. Gomes, J.F. Mano, R.L. Reis,  $\beta$ -PVDF membranes induce cellular proliferation and differentiation in static and dynamic conditions, *Mater. Sci. Forum* 587–588 (2008) 72–76.
- [238] J. Reis, C. Frias, C. Canto, E. Castro, M.L. Botelho, A.T. Marques, J.A.O. Simoes, F. Capela, E. Silva, J. Potes, A new piezoelectric actuator induces bone formation *in vivo*: a preliminary study, *J. Biomed. Biotechnol.* 2012 (2012) 1–7.
- [239] M. Kitsara, A. Blanquer, G. Murillo, V. Humbot, S.D.B. Vieira, C. Nogues, E. Ibanez, J. Esteve, L. Barrios, Permanently hydrophilic, piezoelectric PVDF nanofibrous scaffolds promoting unaided electromechanical stimulation on osteoblasts, *Nanoscale* 11 (2019) 8906–8917.
- [240] S.M. Damaraju, Y. Shen, E. Elele, B. Khusid, A. Eshghinejad, J. Li, M. Jaffe, T. L. Arinze, Three-dimensional piezoelectric fibrous scaffolds selectively promote mesenchymal stem cell differentiation, *Biomaterials* 149 (2017) 51–62.
- [241] B. Callegari, W.D. Belanger, Analysis of the interface formed among the poly(vinylidene fluoride) (piezoelectric and non piezoelectric) and the bone tissue of rats, *Acta Orthop. Bras.* 12 (2004) 160–166.
- [242] J.D. Pereira, R.C. Camargo, C.J. Filho, N. Alves, M.A. Rodriguez-Perez, C. J. Constantino, Biomaterials from blends of fluoropolymers and corn starch-implant and structural aspects, *Mater. Sci. Eng. C* 36 (2014) 226–236.
- [243] H.B. Lopes, T.D.S. Santos, F.S.D. Oliveira, G.P. Freitas, A.L.D. Almeida, R. Gimenes, A.L. Rosa, M.M. Belotti, Poly(vinylidene-trifluoroethylene)/barium titanate composite for *in vivo* support of bone formation, *J. Biomater. Appl.* 29 (2013) 104–112.
- [244] G.G. Genchi, E. Sinibaldi, L. Ceseracciu, M. Labardi, A. Marino, S. Marras, G. DeSimoni, V. Mattoli, G. Ciofani, Ultrasound-activated piezoelectric P(VDFTrFE)/boron nitride nanotube composite films promote differentiation of human SaOS-2 osteoblast-like cells, *Nanomed. Nanotechnol. Biol. Med.* 14 (2017) 2421–2432.
- [245] H. Tamai, K. Igaki, E. Kyo, K. Kosuga, A. Kawashima, S. Matsui, H. Komori, T. Tsuji, S. Motohara, H. Uehata, Initial and 6-month results of biodegradable poly(L-lactic acid coronary stents in humans, *Circulation* 102 (2000) 399–404.
- [246] N. Barroca, P.M. Vilarinho, A.L. Daniel-Da-Silva, A. Wu, M.H. Fernandes, A. Gruber, Protein adsorption on piezoelectric poly(L-lactic) acid thin films by scanning probe microscopy, *Appl. Phys. Lett.* 98 (2011) 133705.
- [247] Y. Ikada, Y. Shikinami, Y. Hara, M. Tagawa, E. Fukada, Enhancement of bone formation by drawn poly(L-lactide), *J. Biomed. Mater. Res.* 30 (1996) 553–558.
- [248] T. Shimono, S. Matsunaga, E. Fukada, T. Hattori, Y. Shikinami, The effects of piezoelectric poly L lactic acid films in promoting ossification *in vivo*, *Vivo* 10 (1996) 471–476.
- [249] Y. Chen, A.F.T. Mak, M. Wang, J. Li, M.S. Wong, PLLA scaffolds with biomimetic apatite coating and biomimetic apatite/collagen composite coating to enhance osteoblast-like cells attachment and activity, *Sur. Coat. Technol.* 201 (2006) 575–580.
- [250] M.P. Prabhakaran, J. Venugopal, S. Ramakrishna, Electrospun nanostructured scaffolds for bone tissue engineering, *Acta Biomater.* 5 (2009) 2884–2893.
- [251] E.K. Ko, S.I. Jeong, N.G. Rim, Y.M. Lee, H. Shin, Bu-Kyu Lee, *In Vitro* osteogenic differentiation of human mesenchymal stem cells and *in vivo* bone formation in composite nanofiber meshes, *Tissue Eng.* 14 (2008) 2108–2119.
- [252] N.M. Neves, A. Kouyumdzhiev, R.L. Reis, The morphology, mechanical properties and ageing behavior of porous injection molded starch-based blends for tissue engineering scaffolding, *Mater. Sci. Eng. C* 25 (2005) 195–200.
- [253] E.J. Bergsma, F.R. Rozema, R.R. Bos, W.C. Debruijn, Foreign body reaction to resorbable poly(L-lactic) bone plates and screws used for the fixation of unstable zygomatic fractures, *J. Oral Maxillofac. Surg.* 51 (1993) 666–670.
- [254] J.C. Middleton, A.J. Tipton, Synthetic biodegradable polymers as orthopedic devices, *1600 Biomaterials* 21 (2000) 2335–2346.
- [255] M. Esmaeili, M.S. Baei, Fabrication of biodegradable polymer nanocomposite from copolymer synthesized by C. necator for bone tissue engineering, *World Appl. Sci. J.* 14 (2011) 106–111.
- [256] Y. Ando, E. Fukada, Piezoelectric properties and molecular motion of poly( $\beta$ -hydroxybutyrate) films, *J. Polym. Sci., Polym. Phys. Ed.* 22 (1984) 1821–1834.
- [257] E. Fukada, History and recent progress in piezoelectric polymers, *IEEE Trans. Ultrason. Ferroelectrics Freq. Contr.* 47 (2000) 1277–1290.
- [258] Y. Wang, Q. Wu, G. Chen, Attachment, proliferation and differentiation of osteoblasts on random biopolyester poly(3-hydroxybutyrate-co-3-hydroxyhexanoate) scaffolds, *Biomaterials* 25 (2004) 669–675.
- [259] Y. Wang, Q. Wu, J. Chen, G. Chen, Evaluation of three-dimensional scaffolds made of blends of hydroxyapatite and poly(3-hydroxybutyrate-co-3-hydroxyhexanoate) for bone reconstruction, *Biomaterials* 26 (2005) 899–904.
- [260] E.I. Pascu, J. Stokes, G.B. McGuinness, Electrosyn composites of PHBV, silk fibroin and nano-hydroxyapatite for bone tissue engineering, *Mater. Sci. Eng. C* 33 (2013) 4905–4916.
- [261] J. Ni, M. Wang, *In vitro* evaluation of hydroxyapatite reinforced polyhydroxybutyrate composite, *Mater. Sci. Eng. C* 20 (2002) 101–109.
- [262] J. Xi, L. Zhang, Z. Zheng, G.Q. Chen, Preparation and evaluation of porous poly(3-hydroxybutyrate-co-3-hydroxyhexanoate)-hydroxyapatite composite scaffolds, *J. Biomater. Appl.* 22 (2008) 293–307.
- [263] L.P. Wu, M. You, D. Wang, G. Peng, Z. Wang, G.Q. Chen, Fabrication of carbon nanotube (CNT)/poly(3-hydroxybutyrate-co-3-hydroxyhexanoate) (PHBHHx) nanocomposite films for human mesenchymal stem cell (hMSC) differentiation, *Polym. Chem.* 4 (2013) 4490–4498.
- [264] B. Kramp, H.E. Bernd, W.A. Schumacher, M. Blynow, W. Schmidt, C. Kunze, D. Behrend, K.P. Schmitz, Poly beta-hydroxybutyric acid (PHB) films and plates in defect covering of the osseous skull in a rabbit model, *Laryngo-Rhino-Otol.* 81 (2002) 351–356.
- [265] G.T. Kose, F. Korkusuz, A. Ozkul, Y. Soysal, T. Ozdemir, C. Yildiz, V. Hasirci, Tissue engineered cartilage on collagen and PHBV matrices, *Biomaterials* 26 (2005) 5187–5197.
- [266] C. Ye, P. Hu, M.X. Ma, Y. Xiang, R.G. Liu, X.W. Shang, PHB/PHBHHx scaffolds and human adipose-derived stemcells for cartilage tissue engineering, *Biomaterials* 30 (2009) 4401–4406.
- [267] K. Zhao, Y. Deng, J.C. Chen, G.Q. Chen, Polyhydroxyalkanoate (PHA) scaffolds with good mechanical properties and biocompatibility, *Biomaterials* 24 (2003) 1041–1045.
- [268] T. Urakami, S. Imagawa, M. Harada, A. Iwamoto, Y. Tokiwa, Development of biodegradable plastic-poly-beta hydroxybutyrate-polycaprolactone blend polymer, *Kobunshi Ronbunshu* 57 (2000) 263–270.
- [269] S.C. Mathur, J.I. Scheinbeim, B.A. Newman, Piezoelectric properties and ferroelectric hysteresis effects in uniaxially stretched nylon-11 films, *J. Appl. Phys.* 56 (1984) 2419–2425.
- [270] H. Wang, Y. Li, Y. Zuo, J. Li, S. Ma, L. Cheng, Biocompatibility and osteogenesis of biomimetic nano-hydroxyapatite/polyamide composite scaffolds for bone tissue engineering, *Biomaterials* 25 (2007) 3338–3348.
- [271] F. You, Y. Li, Q. Zou, Y. Zuo, M. Lu, X. Chen, J. Li, Fabrication and osteogenesis of a porous nanohydroxyapatite/polyamide scaffold with an anisotropic architecture, *ACS Biomater. Sci. Eng.* 1 (2015) 825–833.
- [272] M. Ramu, M. Ananthasubramanian, T. Kumaresan, R. Gandhinathan, S. Jothi, Optimization of the configuration of porous bone scaffolds made of Polyamide/Hydroxyapatite composites using Selective Laser Sintering for tissue engineering applications, *Bio Med. Mater. Eng.* 29 (2018) 739–755.
- [273] L. Cheng, Y. Li, Y. Zuo, J. Li, H. Wang, Nano-hydroxyapatite/polyamide 6 scaffold as potential tissue engineered bone substitutes, *Mater. Res. Innovat.* 12 (2008) 192–199.
- [274] B. Qiao, J. Li, Q. Zhu, S. Guo, X. Qi, W. Li, J. Wu, Y. Liu, D. Jiang, Bone plate composed of a ternary nano-hydroxyapatite/polyamide 66/glass fiber composite: biomechanical properties and biocompatibility, *Internat. j. nanomedic.* 9 (2014) 1423–1432.
- [275] B.K. Shrestha, H.M. Mousa, A.P. Tiwari, S.W. Ko, C.H. Park, C.S. Kim, Development of polyamide-6,6/chitosan electrospun hybrid nanofibrous scaffolds for tissue engineering application, *Carbohydr. Polym.* 148 (2016) 107–114.
- [276] Y. Ando, E. Fukada, M.G. Glymcher, Piezoelectricity of chitin in lobster shell and apodeme, *Biorheology* 14 (1977) 175–179.
- [277] K. Nishinari, E. Fukada, Viscoelastic, dielectric and piezoelectric behavior of solid amylose, *J. Polym. Sci. Phys.* 18 (1980) 1609–1619.
- [278] D. Puppi, F. Chiellini, A.M. Piras, E. Chiellini, Polymeric materials for bone and cartilage repair, *Prog. Polym. Sci.* 35 (2010) 403–440.
- [279] L.B. Rocha, G. Goisis, M.A. Rossi, Biocompatibility of anionic collagen matrix as scaffold for bone healing, *Biomaterials* 23 (2002) 449–456.
- [280] P.L. Moreira, Y.H. An, A.R. Santos, S.C. Genari, *In vitro* analysis of anionic collagen scaffolds for bone repair, *J. Biomed. Mater. Res.* 71B (2004) 229–237.
- [281] N.E. Adel Elkasabgy, A.A. Mahmoud, R.N. Shamma, Determination of cytocompatibility and osteogenesis properties of in-situ forming collagen based scaffolds loaded with bone synthesizing drug for bone tissue engineering, *Internat. J. Poly. Mater.* 67 (2017) 494–500.

- [282] N. Kakudo, A. Shimotsuma, S. Miyake, S. Kushida, K. Kusumoto, Bone tissue engineering using human adipose-derived stem cells and honeycomb collagen scaffold, *J. Biomed. Mater. Res.* 84 (2008) 191–197.
- [283] H.W. Kim, J. Song, H.J. Kim, Bioactive glass nanofiber-collagen nanocomposite as a novel bone regeneration matrix, *J. Biomed. Mater. Res.* 79 (2006) 698–705.
- [284] P. Angele, J. Abke, R. Kujat, H. Faltermeier, D. Schumann, M. Nerlich, B. Kinner, C. Englert, Z. Ruszczak, R. Mehri, R. Mueller, Influence of different collagen species on physicochemical properties of crosslinked collagen matrices, *Biomaterials* 25 (2004) 2831–2841.